Title

Climatic and non-climatic vegetation cover changes in the rangelands of Africa

Authors

Francesco D'Adamo[1]*, Booker Ogutu[1], Martin Brandt[2], Guy Schurgers[2] and Jadunandan Dash[1]

Affiliations

[1]School of Geography and Environmental Sciences, University of Southampton, SO171BJ Southampton, United Kingdom.

[2]Department of Geosciences and Natural Resource Management, University of Copenhagen, 1350 Copenhagen, Denmark.

Corresponding author

*email: f.dadamo@soton.ac.uk

Abstract

About 21% of the African population directly depends on rangeland resources. As this number is predicted to grow, it is important to understand the response of African rangelands to global environmental change and formulate, in turn, better hypotheses on their capacity to support livelihoods. Here we used three decades of satellite data and a dynamic global vegetation model to study the response of rangeland vegetation to recent climate change and to describe changes in the vegetation structure accompanying greening and browning trends. Long-term climate change was the dominant driver of vegetation dynamics in ca. 2,495,000 km^2 of African rangelands (22.7% of the total extent). Examples of these rangelands are in Mauritania, Senegal, Chad, Namibia, Botswana, and South Africa, where the vegetation greened up due to an overall increase in trees, shrubs, and short herbaceous vegetation. We further identified a more extended different type of rangeland (ca. 2,915,000 km^2) where vegetation dynamics appeared to be largely unrelated to long-term climate variations. In these rangelands, we observed opposite trends between woody cover (trees and shrubs) and short vegetation (mostly representative of the herbaceous layer). Greening (West Africa, South Sudan) was associated with an overall increase in woody cover (+4.4%) and a concomitant decline in short vegetation (-3.4%), while browning (Angola, Mozambique) resulted from a decrease in woody cover (-2.6%) and an increase in short vegetation (+4.3%) (total per cent change average during 1982-2015). Our results offer a nuanced perspective to frame greening and browning trends in rangeland systems. While greening may mitigate climate change via higher carbon uptake, the encroachment of less palatable woody species reduces the resources available to pastoral communities. On the other hand, browning due to a reduction in the woody cover attenuates carbon sequestration rates, but the observed increase in short herbaceous vegetation may hint a relative increase in forage resources.

Keywords

Rangeland dynamic, vegetation composition, remote sensing, DGVM, trend analysis, pastoral welfare

1 Introduction

The International Grassland Congress and the International Rangeland Congress defined rangelands as domestic or wildlife grazing lands generally including grasslands, woodlands, shrublands, and some extent of deserts (Allen et al., 2011). Estimates of the proportion of Africa's land covered by rangeland range from ca. 22,000,000 km² (Flintan, 2012), ca. 14,500,000 km² (White et al., 2000), ca. 13,000,000 km² (Hoffman and Vogel, 2008), ca. 8,100,000 km² (Ellis et al., 2010), to ca. 6,700,000 km² (Dixon et al., 2001) (depending on definitions and data sources). They provide the primary (e.g., meat, bones, hide) and secondary (e.g., milk, manure, fibre, wool, traction, eggs) animal products for the livestock rearing activities of some 270,000,000 people, both pastoralists and agro-pastoralists (FAO, 2017; Phelps and Kaplan, 2017). Other ecosystem services supplied by rangelands include the provision of water resources, shade, heritage and recreation, wildlife habitat conservation, and carbon sequestration (Lal, 2004; Sala et al., 2017).

The dependency on African rangeland resources is expected to grow due to the estimated increase of the African population to double by 2050 (UN DESA, 2019). Principally, this implies that livestock products will be increasingly transported to urban (i.e., non-rangeland) areas and will accelerate rangelands conversion to croplands to meet the food demand (Alkemade et al., 2013; van Ittersum et al., 2016). However, the opposite is also possible, since deforestation and the rural-urban migration (i.e., farmland abandonment) may foster the creation of new rangeland-type spaces (Benayas et al., 2007; Bond and Zaloumis, 2016). In addition to increasing social demands, the future of rangelands will also depend on the impacts of rising temperature and changes in the distribution and intensity of climate extremes (Kharin et al., 2007; Niang et al., 2014). For instance, although large disagreements still exist on the response of African ecosystems to different climate change scenarios (Midgley and Bond, 2015), drought may become more severe and frequent in southern and western Africa (Gizaw and Gan, 2017), while in eastern Africa this appears to be happening already (Nicholson, 2016). Similarly, recent studies have linked short-term shifts in rainfall patterns (Brandt et al., 2019; Zhang et al., 2019), rising levels of atmospheric CO_2 (Stevens et al., 2016; Wigley et al., 2010), or significant declines in large mammals (Daskin et al., 2016) to woody encroachment in African savannas. The persistence of drier and warmer conditions and shifts in the vegetation composition represents a major risk not only for the regular food security of rangeland communities (Thornton et al., 2009), but also for rangeland biodiversity richness and carbon stock dynamics (Bond, 2016; Lange et al., 2015).

One way to better understand how future climate change will influence the rangelands of Africa is to evaluate historical data to assess how the vegetation has responded to climate in the past. However, despite the increasing availability of global long-term satellite data, this information is still not readily available. In fact, while the vegetation of Africa is reported to be largely sensitive to water availability (mostly in arid and semi-arid environments) (Anyamba et al., 2014; Herrmann et al., 2005; Moncrieff et al., 2016) or recent CO_2 fertilization (tropical regions) (Nemani et al., 2003; Zhu et al., 2016), many non-climatic disturbances influence its dynamics at different spatiotemporal scales. These may include land-use change and fragmentation (Hobbs et al., 2008; Song et al., 2018), land management (Kiage, 2013; Stevens et al., 2016), armed conflicts (Bromley, 2010; Gorsevski et al., 2012), or infrastructure (Dobson et al., 2010), among others. Thus, the location and extent of the African rangelands where climate is the predominant or subordinate driver of long-term vegetation dynamics are nowadays unclear. Relevant to this conundrum are ecological studies assessing what limits savanna boundaries and the tree-grass coexistence. These have explained that a world without fire would be forest-dominated (Bond et al., 2005), or that forests prevail in regions receiving more than 2,500 mm/yr of rainfall while grass-dominated systems occur below 650 mm/yr (Sankaran et al., 2005), 750 mm/yr (Hirota et al., 2011) or 1000 mm/yr (Staver et al., 2011). Between these end members, ecosystems can persist as either forest or savanna depending on rainfall seasonality and disturbances (e.g., fire, mammalian herbivory) (Mayer and Khalyani, 2011). For instance, fire suppression would promote woody plant and canopy closure, which reduces light and hence grasses (that in turn reduces fire), while a strong rainfall seasonality would enhance fuel curing, fire frequency, open canopy and therefore a light-demanding grass state (that in turn favours fire) (Lehmann et al., 2011; Oliveras and Malhi, 2016; Pausas and Bond, 2020). However, accounting for spatial and temporal inter-relationships between these elements remains complex and still represents a barrier to our understanding of potential future biome shifts (Wei et al., 2020). Remote sensing studies have tried to overcome such complexity by focusing on the dynamics of one specific structural component of the vegetation, i.e. woody plants. Not only this is because the phenomenon of "woody plant encroachment" came into the spotlight of recent research (e.g., Axelsson and Hanan, 2018; Brandt et al., 2020; Li et al., 2020; Skowno et al., 2017; Stevens et al., 2016; Venter et al., 2018), but also because long-term assessments of woody vegetation dynamics were made feasible by new data such as vegetation optical depth (Andela et al., 2013; Brandt et al., 2017). As a consequence, less is known about long-term changes in the short vegetation layer and the relative availability of herbaceous plants. It is however important to better understand the dynamics of all vegetation layers to formulate appropriate hypotheses on the current and future provision of ecosystem services from rangelands as well as to improve our knowledge on rangeland carbon dynamics. Building on the existing knowledge of woody vegetation dynamics, our study includes an assessment of short vegetation to provide a more comprehensive picture of potential implications associated with long-term changes in rangeland vegetation cover. More specifically, here we (a) identify those rangelands where changes in vegetation greenness were either mostly driven or unaffected by long-term climate change and (b) combine the properties of different satellite data to disentangle these changes in terms of the vegetation structure. By doing so, this study provides a long-term overview of how rangeland natural vegetation cover has changed across Africa in the last three decades.

2 Materials and methods

2.1 Study area

An accurate definition of rangeland would allow to effectively estimate their spatial extent, facilitate the identification of owners or administrators, and yield more appropriate management strategies (Lund, 2007). However, ca. 300 rangeland definitions have been suggested in over a century of rangeland science and, nowadays, this term is still rather nebulous (Reeves et al., 2015). Much of this confusion likely exists because no clear distinction is made between the land use and land cover features or due to the misuse and misclassification of different classes (e.g., woodland, savanna, forest) (Lund, 2007; Phelps and Kaplan, 2017). In turn, this may explain why most terrestrial ecosystem studies have focused on better-defined regions such as drylands or forests. For our purpose, here we focused on observed land cover as defined in the moderate resolution imaging spectroradiometer (MODIS) global land cover product (MCD12C1 collection 6) (Sulla-

Menashe and Friedl, 2018). From this product, we selected only the land cover classes that are typically included within rangeland definitions (Supplementary Fig. S1), i.e., shrublands, savannas, and grasslands, and therefore excluded forests, croplands, wetlands, urban and barren lands. According to this classification, we calculated that rangelands cover 10,999,375 km^2 of the African continent, i.e., 92,500 km^2 of closed shrublands, 1,453,125 km^2 of open shrublands, 574,375 km^2 of woody savannas, 3,236,250 km^2 of savanna, and 5,598,125 km^2 of grasslands (Fig. 1). We acknowledge that this value may best represent the potential rather than actual rangeland extent for Africa given that no land use evidences were included herein. However, for simplicity of terminology, our study area is hereafter referred to as rangeland. Alternative rangeland maps for Africa could be derived from White (1983), a continent-wide potential natural vegetation classification system, or Ellis et al. (2010), who produced an anthropogenic biome classification based on how humans transformed terrestrial biosphere (Supplementary Fig. S2). We opted for the MODIS-based product as the map from White (1983) would likely include extended areas now converted to croplands, while the Ellis et al. (2010) product was shown to be affected by problematic statistical inventory data and land use assumptions (Phelps and Kaplan, 2017; Sayre et al., 2017).

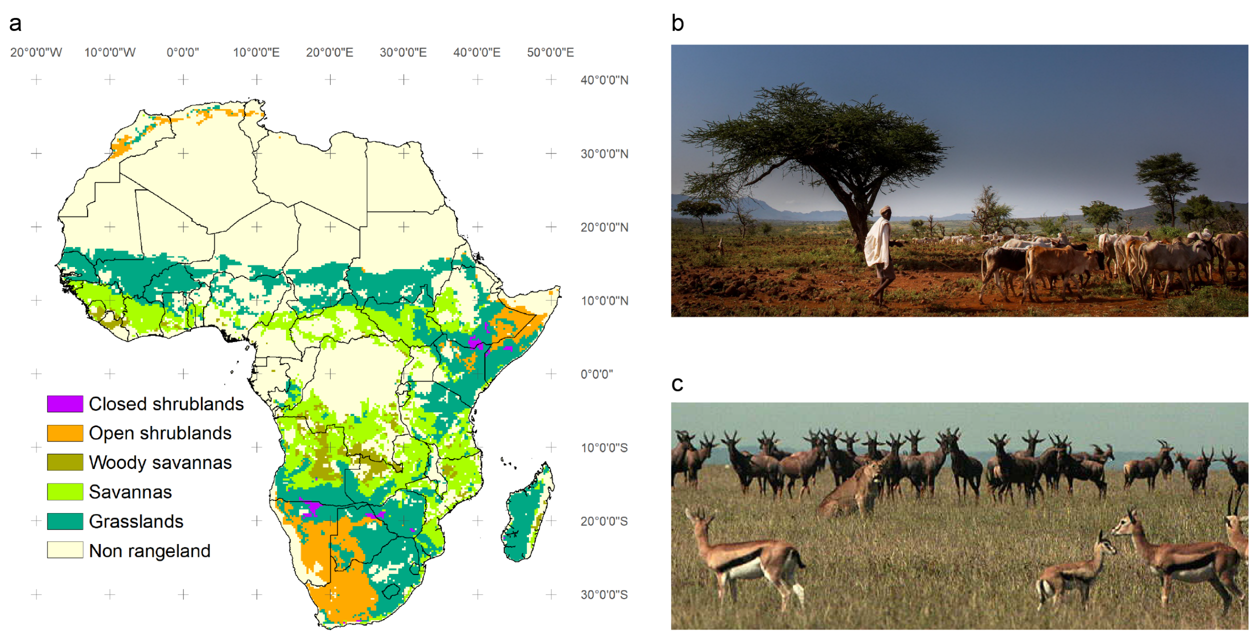

Fig. 1 Rangeland extent derived from the MODIS MCD12C1 collection 6 global land cover product (Sulla-Menashe and Friedl, 2018). The classes follow the International Geosphere-Biosphere Programme (IGBP) classification scheme.

Forests, croplands, wetlands, urban, and barren lands were not included and are indicated as non rangeland (see Supplementary Fig. S1). The extent of ca. 11,000,000 km² fits well within existing rangeland extent estimations for Africa (a). Herdsman and cattle in rangelands of Ethiopia (photo credit: Camille Hanotte, International Livestock Research Institute) (b). Kenya wildlife-rich rangelands (photo credit: Dave Elsworth, International Livestock Research Institute) (c).

2.2 Data sources and preprocessing

Multiple, independent, and complementary datasets should be used to overcome the limitations of individual datasets and reduce uncertainties. To this end, we investigated rangeland dynamics in Africa during 1982-2015 using an ensemble of optical and microwave satellite data as well as a dynamic global vegetation model. Given the differences in the nominal spatial resolution, all data were resampled at the common pixel size of 25 km x 25 km using the aggregate and resample functions (bilinear algorithm) from the R package 'raster' (Hijmans et al., 2021). We determined annual means over growing season integrated metrics to avoid uncertainties caused by the seasonal complexity that exists throughout Africa. This is a common approach in broad-scale terrestrial ecosystem studies (Fensholt et al., 2009; Helldén and Tottrup, 2008; Mueller et al., 2014). All analyses were performed within the R environment (R Core Team, 2018).

2.2.1 Normalised Difference Vegetation Index (NDVI)

The AVHRR-derived GIMMS NDVI3g.v1 (8 km x 8 km, 1981-2015) (Pinzon and Tucker, 2014) is one of the few datasets enabling vegetation greenness trend analysis over more than 30 years (Forkel et al., 2013). The NDVI3g.v1 comes with three main differences compared to the previous NDVI3g.v0. First, errors in the cross-calibration with SeaWiFS data were addressed to minimize overestimations of NDVI values in sparsely vegetated regions (Burrell et al., 2018). Second, it covers two extra years by integrating data from NOAA-17 and NOAA-18 satellites and, third, the quality flags, three instead of seven, are embedded separately to simplify the use of the dataset. After removing NDVI values that did not represent vegetated areas (NDVI $\leq$ 0), NDVI was further filtered to account for spurious signals due to soil-vegetation spectral mixing, which overestimates vegetation index over both dark-background and, to a lesser extent, bright-background soils typical of rangeland areas (Elvidge and Lyon, 1985; Huete, 1988). Previous studies overcame this issue by masking out values smaller than 0.1 (Bi et al., 2013), 0.15 (Eastman et al., 2013) or 0.2 (Zhu and Southworth, 2013). We tested all these thresholds and eventually chose the threshold at 0.1, as 0.15 and 0.2 would mask out too many rangeland pixels (36% and 48% respectively, only 9% at 0.1). Monthly mean NDVI was then calculated by averaging the two maximum-value composite (MVC) values provided for each month (one for day 1-15 and one for day 16-end of the month per pixel). Instead of averaging, some studies aggregate bi-monthly values using again the MVC approach because it further reduces residual cloud cover effects (Bao et al., 2015; Ibrahim et al., 2015; Zhu and Southworth, 2013). However, this was not necessary as we excluded tropical forests and only used good quality pixels (i.e., flag 0), which refer to NDVI values without apparent issues (e.g., cloud-free pixels). Also, the MVC approach would represent just fifteen days of the month, whilst averaging enabled a more representative mean of a given month. Annual mean NDVI composites were then produced averaging January to December data. However, because good quality pixels did not necessarily represent all months during the time-series, it was essential to check the consistency in the annual availability of good quality pixels. The best-case scenario corresponded to a pixel having a good quality value in every month (i.e., annual mean calculated with 12 values). This case represented 91% of the African rangelands. For the remaining 9%, we conducted a sensitivity analysis aimed at determining the minimum number of months needed to obtain a representative annual mean. Using those pixels with 12-months of good quality data, randomly selected months were progressively removed. We then calculated the difference between the mean obtained with the full and reduced number of months and defined the acceptable number of months as that needed to achieve an average difference $\leq$ 5%. On average, annual mean NDVI composites were calculated with 12 to a minimum of 10 months, meaning that annual mean values calculated with 9 or less good quality pixels produced a difference with the 12-months good quality mean > 5% (Supplementary Fig. S3). In each year, the random approach was changed to ensure that the order in which pixels were removed varied to prevent the introduction of seasonal biases. The R package 'gimms' (Detsch, 2016) was used to download the GIMMS dataset, rasterize the data, and apply the quality flags.

2.2.2 Vegetation Continuous Fields (VCFs)

VCFs (5 km x 5 km, 1982-2016) are produced from the different AVHRR sensors by compiling the fourth version of the Long Term Data Record (LTDR) (Song et al., 2018). Other satellite information derived from MODIS, ETM+, QuickBird, WorldView, IKONOS, and GeoEye was used at different stages of the VCFs realization (e.g., radiometric, atmospheric, and geolocation corrections, conversion of daily LTDR to yearly VCFs, annual metrics normalization, validation) (Song et al., 2018). VCFs include global annual data of tree cover, short vegetation, and bare ground. Tree cover data refer to vegetation taller than 5 m, and it is calculated considering the portion of land covered by the vertical projection of the tree canopy (Song et al., 2018). Tree cover is not synonymous of forest cover, but it can be used to classify an area as forested or non-forested (depending on the size of the area and the amount of surface covered by trees taller than 5 m). Short vegetation data include crops, herbaceous vegetation, shrubs, and mosses, while bare ground data represents non-vegetated areas. Every pixel reports the percentage of tree cover, short vegetation, and bare ground at the peak of the local growing season (i.e., each pixel sums up to a value of 100). Applying established validation protocols, the accuracy of the VCFs data was assessed in 475 locations globally using the best long-term reference datasets currently available, i.e., the Landsat-derived VCFs and the United States Geological Survey (USGS) tree cover reference database (Pengra et al., 2015). For all combinations (i.e., AVHRR TC vs. Landsat TC, AVHRR SV vs. Landsat SV, AVHRR BG vs. Landsat BG, and AVHRR TC vs. USGS TC), Song et al. (2018) calculated an overall accuracy higher than 90%, and a mean absolute error comprised between 4.4% (AVHRR BG vs. Landsat BG) and 9.9% (AVHRR TC vs. USGS TC). It is however hard to assess how these uncertainties may affect the spatial distribution of long-term trends in tree cover, short vegetation, and bare ground. This is because the mean absolute error provided is obtained from a global validation (i.e., averaging the errors in each location used for the validation) and therefore the error is not spatially explicit. No data are available for 1994 and 2000 due to the lack of data in the LTDR. Hereafter, tree cover refers only to the woody component of the Song et al. (2018) datasets, while woody cover refers to woody vegetation as a whole.

2.2.3 Vegetation Optical Depth (VOD)

VOD retrievals (25 km x 25 km, 1992-2011) (Liu et al., 2015) are derived from passive microwave observations which are insensitive to cloud cover and atmospheric contamination (Brandt et al., 2017). The VOD signal is sensitive to the total water content of all plant components in the upper canopy layer, which include leaves, stems, and branches (Tian et al., 2017). It is described by a negative exponential function of the transmissivity of vegetation and represents a dimensionless measure of how much of the microwave radiation emitted by the soils and the vegetation is attenuated by the vegetation itself (Liu et al., 2011). In other words, VOD tends towards zero when the transmissivity is one, meaning that no microwave energy is attenuated by soil or vegetation. This is the case of bare soils. Vice versa, VOD reaches maximum values when the transmissivity is zero, which happens when most microwave emissions are attenuated by vegetation. This is the case of densely vegetated areas (Liu et al., 2011). The VOD dataset used in this study was created merging passive microwave observations from three sensors (i.e., SSM/I, AMSR-E, and WindSat radiometers) (Liu et al., 2015), using the NASA and Vrije Universiteit Amsterdam land parameter retrieval radiative transfer model (Meesters et al., 2005; Owe et al., 2008). Recent studies testing the consistency of VOD during 1992-2011 showed that no errors occurred at the time of sensor shifts thanks to the long overlapping period existing between the SSM/I, AMSR-E, and WindSat instruments (Tian et al., 2016). Here we used annual minimum VOD from monthly data to reduce the contribution of herbaceous vegetation and apply these data as a proxy for woody cover (Brandt et al., 2019, 2017). Annual minimum VOD was also used as a proxy for aboveground standing biomass given its ability to detect the biomass signal (Liu et al., 2011; Owe et al., 2001). Since both NDVI and VCFs data are derived from optical AVHRR data, VOD represented an independent microwave data stream.

2.2.4 Precipitation

The CHIRPSv2.0 precipitation dataset (5 km x 5 km, 1981-present) (Funk et al., 2015) was produced from microwave, infrared, reanalysis, and gauge data. In summary, the Climate Hazard Precipitation Climatology (CHPclim), which represents a historical precipitation climatology created from different physiographic rainfall indicators and monthly long-term estimates of rainfall, brightness temperature, and land surface temperature, is multiplied with infrared precipitation estimates (IRP) obtained from a regression model of cold cloud duration. This unbiased gridded rainfall product, known as the Climate Hazards Group IR Precipitation (CHIRP), is blended with ground station data into the CHIRPS product using a per-pixel inverse distance weighted average algorithm based on the five spatially closets stations to each CHIRP gridded location (Funk et al., 2014). Information about the uncertainty of this algorithm is yet unavailable (Funk et al., 2015). CHIRPS provides rainfall in millimetres per month and comes with no missing data. Annual mean rainfall composites were built by averaging December to the following November data (i.e., one-month lag). This is because rainfall effects on vegetation are not immediate and, generally, the water of the previous month influences plants more than the water of the current month (Papagiannopoulou et al., 2017; Svoray and Karnieli, 2011). However, we also tested no lag composites (i.e., averaging same-year January to December data) and found them to be significantly similar to the one-month lag composites (Supplementary Fig. S4).

2.2.5 Soil moisture

ESA CCI data fulfil the need for a long-term multi-satellite soil moisture product (Dorigo et al., 2017), and it represents the only available dataset able to span the time-series of this study. The ESA CCI v04.2 soil moisture dataset (25 km x 25 km, 1978-2016) is available as an active, passive, or active-passive merged product. Active observations are derived from AMI-WS and ASCAT scatterometers, the passive from seven different radiometers (SMMR, SSM/I, TMI, AMSR-E, WindSat, AMSR2, SMOS). Here we used the merged dataset because it brings together the advantages of active observations, better performing on medium to densely vegetated areas, and passive ones, which are more precise over sparse vegetation and can better discriminate between dry and wet soils (Chung et al., 2018a; Dorigo et al., 2010; Dorigo et al., 2017). The merging scheme is different from all other versions. While, previously, active and passive observations were firstly merged in one single active and one single passive product and later converted together in the final merged dataset (Chung et al., 2018b), in the v04.2 all active and passive datasets are weighted-average blended into the combined product in one single step to reduce uncertainties (Gruber et al., 2019). ESA CCI soil moisture data are provided in volumetric unit (m^3 m^{-3}). Common practice assumes that satellite soil moisture data refer to the first 5 cm of soil (Dorigo et al., 2010). More confidence on deeper soil moisture content was given by a study showing a significant correlation between remotely sensed soil moisture data of the upper 5 cm and ground-based observations within the first 10 cm (Dorigo et al., 2015), yet the impact of soil moisture on plants that can access water beyond this depth may be underestimated. Further, we noticed that some pixels have uncertainties higher than the actual soil moisture signal. This is because the way uncertainties are estimated (i.e., triple collocation analysis and error propagation), may not converge to a robust estimate either in case only a few observations were available or when the signals from different datasets diverged significantly (Chung et al., 2018b). For this reason, the soil moisture signal may still be relatively accurate even if it is lower than the uncertainty (Dorigo, personal communication, 2019). Due to the scarcity in good quality soil moisture data between 1982 and 1991 (only two operational radiometers, i.e., SMMR and SSM/I) and between 2003 and 2006 (ERS-2 on-board storage failure) (Dorigo et al., 2017), we increased the coverage of soil moisture values by aggregating all available daily flag 0 pixels to monthly level (McNally et al., 2015). Annual mean soil moisture composites were then created applying the same sensitivity analysis used to calculate annual mean NDVI composites (at least 9 months were needed to have a difference with the full 12-months good quality mean $\leq$ 5%) (see section 2.2.1).

2.2.6 Simulated biomass carbon

The dynamic global vegetation model LPJ-GUESS simulates how the structure and function of ecosystems vary in response to changes in environmental conditions (Smith et al., 2014, 2001). The model simulates the per-pixel composition of vegetation fractional coverage as a combination of twelve possible plant functional types (PFTs), ten woody and two grassy (Sitch et al., 2003; Smith et al., 2014). Here we simulated the PFT composition as per biomass carbon, which is represented by leaves, roots, sapwood, and heartwood carbon pools (i.e., the four pools where the living biomass is distributed). Total aboveground carbon (AGC) was computed as the sum of leaves, sapwood, and heartwood, while woody biomass carbon (WDC) is calculated by adding sapwood and heartwood only. WDC thus represents the woody carbon content and relates to woody cover (Brandt et al., 2017). To bring the model from the initial condition (i.e., landscape with no vegetation) to a steady state at the start of the subsequent scenario phase (here 1st January 1901), we run a 500 years spin-up phase consisting in the iterative application of the first 30 years of the input climate variables. Later, our 1982-2015 simulations at 50 km spatial resolution were based on environmental conditions that included monthly climate data of temperature, precipitation and sunshine duration from the Climate Research Unit, version TS 3.24.01 (Harris et al., 2014), estimates of monthly nitrogen deposition (Lamarque et al., 2013), and ice-core and flask measurement derived annual mean atmospheric CO_2 data (Etheridge et al., 1996). Given that these climate data are unrelated to the CHIRPS and ESA CCI, we could evaluate our results by means of distinct products. Because we were interested in the vegetation dynamic of rangelands, which are regions dominated by natural vegetation, LPJ-GUESS simulations did not take into account any human influences such as land use or land-use change (Tong et al., 2018). The uncertainties in these simulations originate from processes that are lacking or poorly parameterised in the model, as well as from error propagation through erroneous environmental forcing data and spatial and temporal averaging in these. However, LPJ-GUESS has been shown to capture the interannual variability of the terrestrial uptake of CO_2 at the global scale (Ahlström et al., 2015; Piao et al., 2013; Schurgers et al., 2018) and, more specifically, the interannual and decadal dynamics of biomass changes in Africa (Brandt et al., 2018, 2017; Lehsten et al., 2009; Sallaba et al., 2017), both of which are primarily driven by climatic variations. This gives us confidence in using LPJ-GUESS as a tool to estimate expected climate-driven trends in this study.

2.3 Analysis

Our analysis aimed to understand the response of rangeland natural vegetation cover to recent climate change and to describe greening and browning as per changes in the structural component of the vegetation. We did this in three consecutive steps. First, we defined long-term changes in vegetation greenness (i.e., GIMMS NDVI). Second, we established the spatiotemporal relationship between these changes in vegetation greenness and water availability represented by precipitation and soil moisture. Third, we assessed five other climate variables affecting plant growth by employing the LPJ-GUESS simulated biomass carbon data and used VOD and VCFs to discern between woody and short herbaceous vegetation.

2.3.1 *Trends in vegetation greenness*

A per-pixel trend analysis allowed us to statistically evaluate whether in each pixel there was a monotonic increase or decrease in vegetation greenness over time. Linear trends were obtained by calculating the slope of the regression of annual mean NDVI composites during 1982-2015 ($n = 34$). The non-parametric Spearman's rank test was used to calculate the significance of the trends at the 95% level ($p < 0.05$).

2.3.2 *Relationship between vegetation greenness and water availability*

It is well established that plant growth in arid and semi-arid areas is largely limited by water availability (Fensholt et al., 2012). Because ca. 65.5% of African rangelands occur within arid and semi-arid regions (Supplementary Fig. S5), we were first interested in understanding how much of the observed trends in vegetation greenness can be explained by changes in precipitation and soil moisture. To this end, we started by calculating and mapping the per-pixel Spearman's rank correlation coefficient (ρ) between NDVI and precipitation, and between NDVI and soil moisture during 1982-2015 ($p < 0.05$). These two maps described the spatiotemporal relationship between vegetation greenness and water availability. Similar to previous studies (Andela et al., 2013; Hoscilo et al., 2015), we then assessed whether an increase or decrease in vegetation greenness was attributable to changes in precipitation or soil moisture by extracting pixels with significant trends in NDVI as well as significant relationships between NDVI and water availability. Thus, these pixels identify rangelands where NDVI, precipitation, and soil moisture increased or decreased together during 1982-2015, while the remaining pixels identify rangelands where this relationship was missing. While we only discussed statistically significant relationships, we acknowledged that some relationships between NDVI, rainfall, and soil moisture may be insignificant due to some unavoidable data uncertainties.

2.3.3 *Rangeland vegetation cover dynamics*

To define greening and browning trends as either controlled or unrelated to climate variability, other climate variables must be assessed in addition to water availability. The LPJ-GUESS model, which is able to detect more complex climate dynamics (e.g., higher temperature combined with changes in precipitation patterns) than correlation analyses (Sitch et al., 2003), was used to check whether the full set of its climatic drivers (i.e., temperature, precipitation, sunshine duration, nitrogen deposition, and CO_2 concentration) could reproduce the observed changes in vegetation greenness assuming that greening/browning trends should relate to an increase/decrease in the simulated biomass carbon. In addition, we looked at trends in VOD given that, despite the shorter time-series (1992-2011 vs. 1982-2015), VOD was shown to provide clear indications of aboveground biomass carbon (Liu et al., 2015). Therefore, we defined changes in vegetation greenness as climatic if VOD, NDVI, AGC, and WDC showed concomitant and comparable trends during 1982-2015 (i.e., LPJ-GUESS could reproduce changes in vegetation based on climate variables), and areas of disagreement between trends in NDVI and VOD and trends in AGC and WDC were described as non-climatic. While intermediate conditions still exist at different spatiotemporal scales (e.g., disturbances such as fire to affect climatic rangeland dynamics or changes in precipitation regimes affecting non-climatic rangeland dynamics), this change attribution approach still allowed us to identify, at an annual timescale, those areas where long-term climate was the main or subordinate driver of vegetation dynamics. Finally, we moved beyond the simple greening and browning label by using VCF and VOD data to decompose changes in NDVI into the woody and short components of the vegetation. While the tree cover data by Song et al. (2018) map only trees taller than 5 m, the annual minimum VOD signal includes also small trees and shrubs (Brandt et al., 2019). This aspect is decisive as the combined use of these two products allowed our analysis to fully represent the general rangeland woody cover community. Noticeably, shrubs are part of both VOD and short vegetation signals, yet we believe these woody species to be better detected by the VOD signal given the more extensive evidence of VOD to well represent woody plants regardless of their size or canopy closure (Brandt et al., 2017, 2016; Liu et al., 2015; Tian et al., 2017). Also, as herbaceous-shrub interactions occur at a much higher spatial resolution than most long-term remote sensing products, the full disaggregation of rangeland vegetation into its shrubby and herbaceous component is challenging. As we did not consider croplands in the analysis (see section 2.1), we ultimately assumed short vegetation data to remain largely representative of short non-woody herbaceous species.

Methodologically, we used standardised anomalies calculated with the z-score formula, i.e., z-score = (value – mean) / standard deviation (dimensionless). Standardising is an effective approach to convert different scales to the same comparable scale, and it tells, for each pixel value, the number of standard deviation away from its time-series mean (i.e., anomaly) (Helldén and Tottrup, 2008). Standardised anomalies in VOD, VCFs, AGC, and WDC were calculated in those rangelands previously characterised in relation to water availability alone (i.e., section 2.3.2). To represent the time-series, we then averaged all per-pixel standardised anomalies in every year and presented the results showing the slope of the regression of these anomalies expressed as total per cent change during 1982-2015 (1992-2011 for VOD).

3 Results

3.1 Trends in vegetation greenness

Significant linear trends ($p < 0.05$) in vegetation greenness were observed in approximately half of African rangelands (ca. 5,410,000 km^2) between 1982-2015. Approximately 4,140,000 km^2 of these changes were positive (i.e., greening) and mostly occurred across the Sahel, West Africa, Chad, South Sudan, Namibia, Botswana, and South Africa. Negative trends (i.e., browning) were mostly clustered in Angola and Mozambique, yet their extent was significantly smaller (ca. 1,270,000 km^2) compared to the greening areas (Fig. 2).

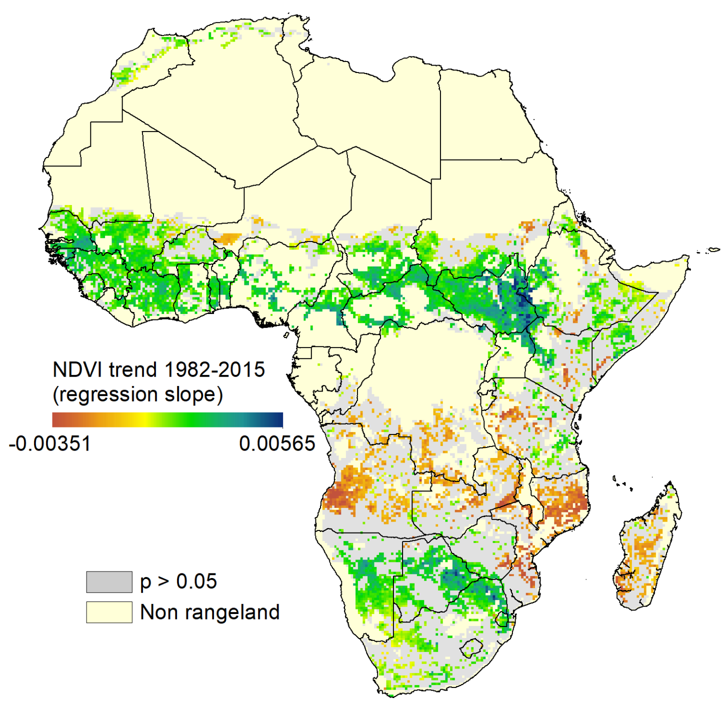

Fig. 2 Trends in vegetation greenness in rangelands during 1982-2015 as indicated by the GIMMS3g.v1 NDVI

(NDVI unit yr[-1]). Trends over time were indicated by the slope of the regression ($n = 34$, Spearman's rank test, $p < 0.05$). Vegetation greenness overall increased (6,623 pixels) between 1982 and 2015 (browning accounted for 2,030 pixels). Supplementary Figs. S6 and S7 report the trends in vegetation greenness for the African rangelands as derived from the White (1983) and Ellis et al. (2010) maps.

3.2 Relationship between vegetation greenness and water availability

The relationship between annual mean NDVI and annual mean precipitation (Fig. 3a) and between annual mean NDVI and annual mean soil moisture (Fig. 3b) displayed similar outputs. In both cases, statistically significant ($p < 0.05$) correlation coefficients showed a comparable positive strength ($\rho = 0.567$ and $\rho = 0.546$, average) and covered the same regions (northwestern Maghreb, western Sahel, southern Chad, eastern Africa, Namibia, Botswana, and South Africa).

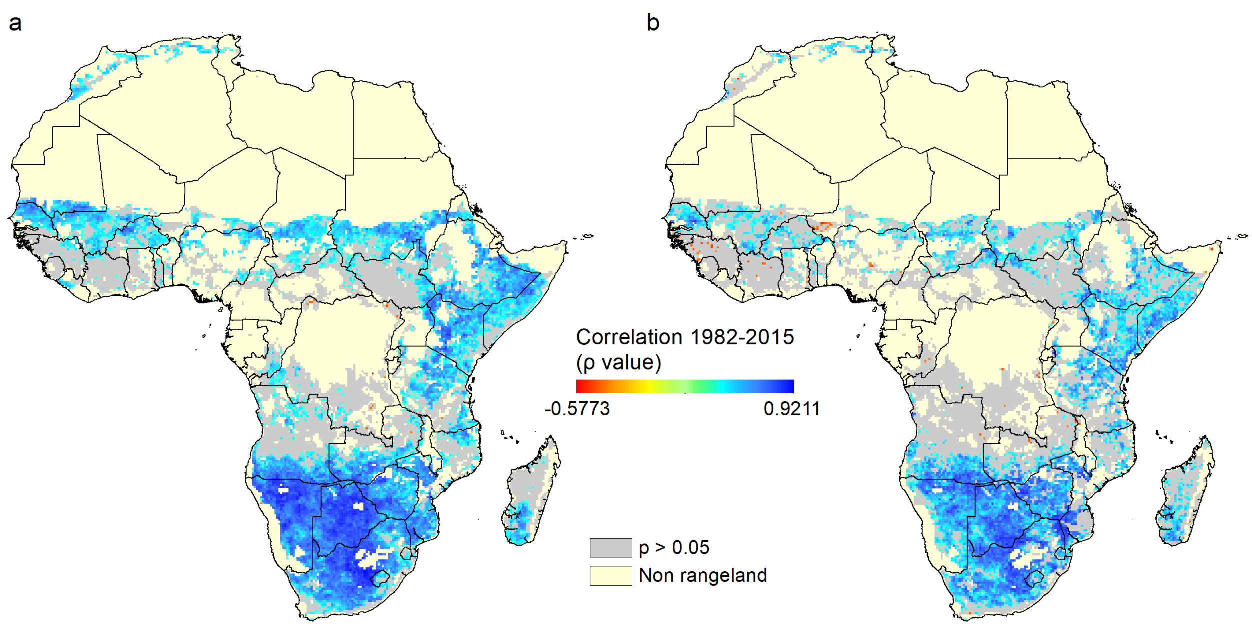

Fig. 3 Relationship between the GIMMS3g.v1 NDVI and CHIRPSv2.0 precipitation (a), and between the GIMMS3g.v1 NDVI and ESA CCIv04.2 soil moisture (b). Long-term relationships were defined by per-pixel Spearman's rank correlation coefficients (ρ) calculated on annual mean composite during 1982-2015 ($p < 0.05$). The NDVI-precipitation (a) and NDVI-soil moisture (b) relationships were significantly similar in terms of strength, type, and spatial distribution. Total pixel count: 10,586 positive vs. 16 negative (a), and 7,628 positive vs. 71 negative (b). Supplementary Figs. S6 and S7 report the relationships between NDVI and precipitation/soil moisture for the African

rangelands as derived from the White (1983) and Ellis et al. (2010) maps.

Statistically significant pixels of these correlation coefficient maps that also showed statistically significant greening and browning trends (i.e., Fig. 2) represented rangeland systems where vegetation was mostly controlled by long-term changes in precipitation and soil moisture (Fig. 4, turquoise and purple shaded areas). Greening (ca. 2,110,000 km^2) was mostly observed in three similar arid and semi-arid regions, i.e., southern Mauritania, Senegal, Mali (hereafter western Sahel), Chad, and Namibia, Botswana, South Africa (hereafter southern Africa), while browning accounted for small and patchy areas totalling ca. 385,000 km^2. Conversely, the remaining pixels (i.e., statistically significant trends in NDVI but no statistically significant correlation between NDVI and water availability) indicated greening and browning largely unrelated to long-term precipitation and soil moisture (Fig. 4, blue and orange shaded areas). Greening (ca. 2,030,000 km^2) was observed in Ghana, Guinea, Ivory Coast (hereafter West Africa), and South Sudan, while browning (ca. 885,000 km^2) was clustered in Angola and Mozambique. In total, ca. 2,915,000 km^2 of the African rangelands (26.5% of the total extent) showed trends in vegetation greenness unrelated to water availability.

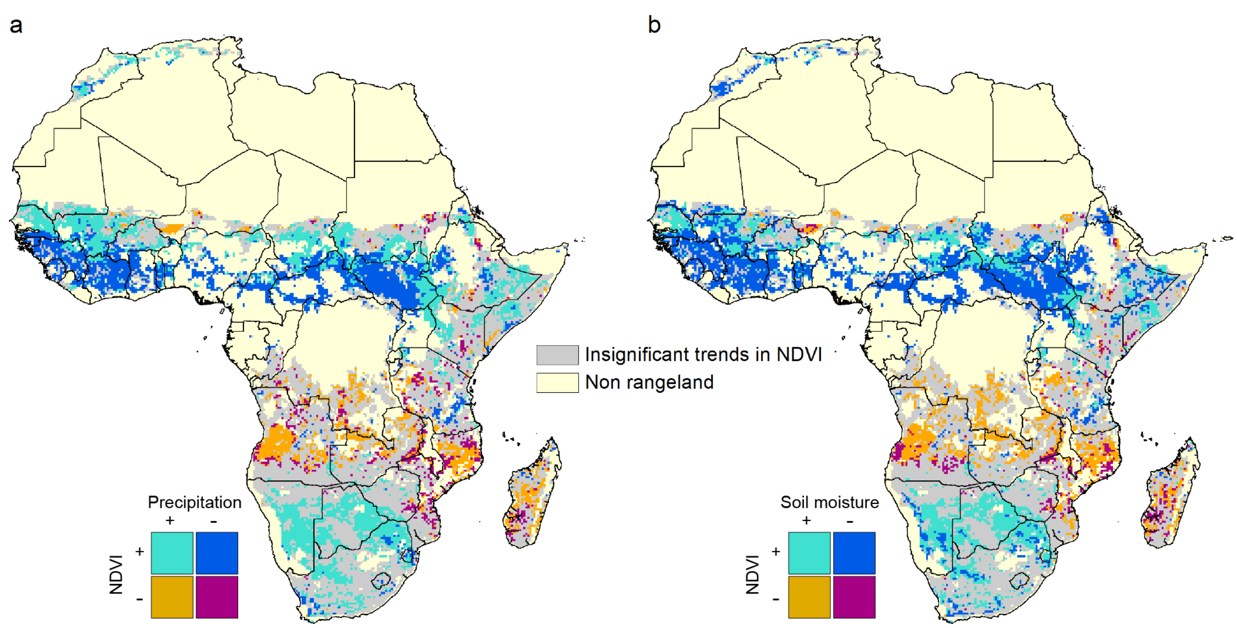

Fig. 4 Co-relationships between trends in NDVI and precipitation (a) and between trends in NDVI and soil moisture (b). NDVI increased together with precipitation and soil moisture across parts of western Sahel (southern Mauritania, Senegal, Mali), Chad, and southern Africa (Namibia, Botswana, and South Africa) (turquoise), while no major regions of

browning due to a decrease in precipitation and soil moisture were observed (purple). Changes in NDVI resulted unrelated to changes in water availability mostly in West Africa (Ghana, Guinea, Ivory Coast) and South Sudan (greening; blue), and Angola and Mozambique (browning; orange).

3.3 Rangeland vegetation cover dynamics

Precipitation and soil moisture alone do not provide enough insights into the greenness response to overall climate. At the same time, vegetation greening and browning cannot be necessarily linked to improvement and deterioration of ecosystem conditions, since the provisioning of ecological services strongly depends on the composition of the vegetation. Building on the two types of rangeland identified in Fig. 4, i.e., water-limited rangelands of western Sahel, Chad, and southern Africa (turquoise and purple shaded areas), and non-water limited rangelands of West Africa, South Sudan, Angola, and Mozambique (blue and orange shaded areas), the analysis of ACG, WDC, VOD, and VCFs addressed these gaps (NDVI, precipitation, and soil moisture were also included in the following z-score analyses).

3.3.1 Vegetation dynamics in the rangelands of western Sahel, Chad, and southern Africa

Western Sahel and Chad showed similar patterns in all indicators (Fig. 5 and Supplementary Fig. S8). Increasing NDVI (5.7% and 6.1%) was associated with a total increase in tree cover (2.0% and 4.7%), VOD (8.0% and 9.6%), and short vegetation (2.4% and 5.1%) during 1982-2015. Bare ground counterbalanced these changes decreasing by 5.5% and 5.7% respectively. The AGC simulations from LPJ-GUESS reproduced the positive changes in NDVI, tree cover, and short vegetation (2.4% and 2.3%), while WDC increased at a comparable rate (1.6%) only in Chad (-0.3% in western Sahel). Similar results were observed in southern Africa (Fig. 5 and Supplementary Fig. S9). Most satellite data (i.e., NDVI 5.0%, VOD 10.6%, short vegetation 2.4%), simulated AGC (1.6%), and precipitation (2.0%) showed a positive trend, while WDC remained unchanged reproducing trends in tree cover (-0.5%).

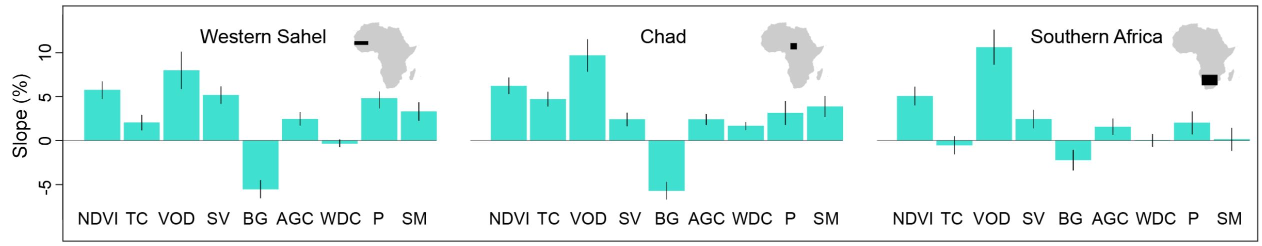

Fig. 5 Vegetation dynamics in the climatic rangelands of western Sahel (southern Mauritania, Senegal, Mali), Chad, and southern Africa (Namibia, Botswana, and South Africa), as indicated by the slope of the regression of standardised anomalies in normalised difference vegetation index (NDVI), tree cover (TC), vegetation optical depth (VOD), short vegetation (SV), bare ground (BG), simulated aboveground carbon (AGC), simulated woody biomass carbon (WDC), precipitation (P), and soil moisture (SM). All indicators increased in western Sahel and Chad during 1982-2015 (except for bare ground). Some discrepancies were observed in southern African rangelands, where changes in NDVI, AGC, SV, and precipitation were comparable but trends in tree cover and WDC did not reproduce trends in VOD. Black lines indicate standard errors (no significant mask was applied). Slope values are reported as total per cent change during 1982-2015 (1992-2011 for VOD) (see Supplementary Figs. S8 and S9). The colour of the bar plots recalls the turquoise of Fig. 4.

3.3.2 Vegetation dynamics in the rangelands of West Africa, South Sudan, Angola, and Mozambique

Different scenarios were observed in West Africa, South Sudan, Angola, and Mozambique. The greening of both West Africa and South Sudan was associated with increasing woody cover, as shown by positive trends in tree cover (4.3% and 6.0%) and VOD (2.0% and 5.3%) (Fig. 6 and Supplementary Fig. S10). However, here we observed a decline (-3.0% and -3.7%) in short vegetation during 1982-2015, meaning that the key contribution to the greening of vegetation was mostly due to woody plants. To some extent, an increase in tree cover and a concomitant decline in short vegetation may also depict trees that during 1982-2015 grew above the 5 m height threshold. Importantly, AGC and WDC experienced very little change in West Africa (-0.3% and -0.5%) and decreased significantly in South Sudan (-7.5% and -7.8%), implying that LPJ-GUESS was unable to reproduce the greening trend observed from satellite data. Changes in woody cover were also responsible for the browning of Angolan and Mozambican rangelands, yet this was more evident in Mozambique, where trends in tree cover (-5.0%) were in line with trends in VOD (-3.1%), than in Angola (tree cover -3.7% and VOD +1.5%) (Fig. 6 and Supplementary Fig. S11). Noticeably, trends in short vegetation were positive in both regions (3.7% and 5.0%), suggesting that this vegetation is replacing woody cover. Despite the overall browning shown by vegetation data streams, strong positive variations in AGC and WDC were observed in rangelands of Angola (6.2% average), while in Mozambique these were slightly negative (-1.6% average). Therefore, also in these two regions the climate variables used to force LPJ-GUESS failed to reproduce the vegetation browning. Importantly, VOD and short vegetation showing diametrically opposite trends in all four areas implies that shrubs are unlikely to be included in both the VOD and short vegetation signals (e.g., if VOD increases and SV decreases, shrubs increase together with VOD, and the decrease in SV will mostly represent a reduction in the herbaceous layer, and vice versa). This evidence thus reinforced our assumption of VOD to better detect the woody component of the vegetation, with short vegetation data representing the short non-woody cover.

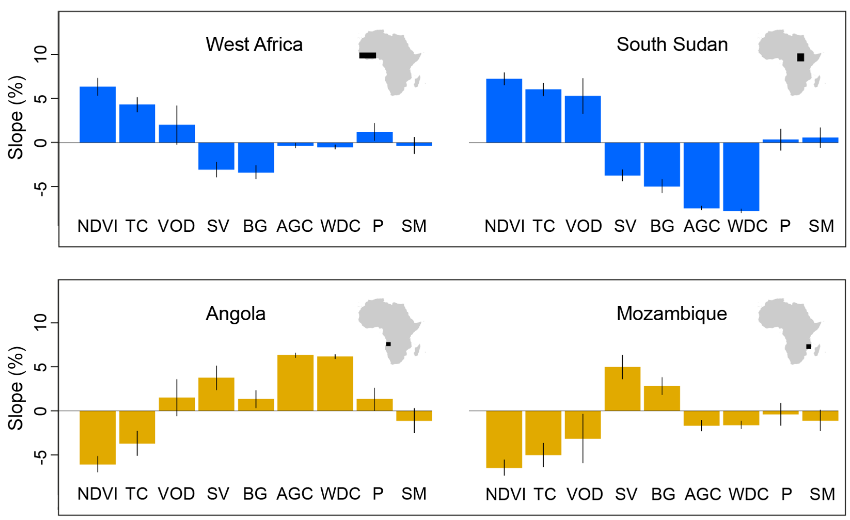

Fig. 6 Vegetation dynamics in the non-climatic rangelands of West Africa (Ghana, Guinea, Ivory Coast), South Sudan, Angola, and Mozambique, as indicated by the slope of the regression of standardised anomalies in normalised difference vegetation index (NDVI), tree cover (TC), vegetation optical depth (VOD), short vegetation (SV), bare ground (BG), simulated aboveground carbon (AGC), simulated woody biomass carbon (WDC), precipitation (P), and soil moisture (SM). The biomass carbon parameters largely failed to reproduce changes in vegetation greenness. Also, woody cover increased where short vegetation decreased (West Africa, South Sudan), and woody cover declined where short vegetation increased (Angola, Mozambique). Black lines indicate standard errors (no significant mask was applied).

Slope values are reported as total per cent change during 1982-2015 (1992-2011 for VOD) (see Supplementary Figs. S10 and S11). The colours of the bar plots recall the blue and orange of Fig. 4.

4 Discussion

The overall greening of the African rangelands during 1982-2015 supports the evidence of a recently greening Earth (Zhu et al., 2016). Regions of vegetation green-up were observed in West Africa, the Sahel, and southern Africa, while vegetation browning was mostly confined in Angola and Mozambique. Vegetation greenness as indicated by NDVI is known to be correlated with vegetation productivity, i.e., a key indicator of measuring land degradation (Abel et al., 2019). Thus, changes in NDVI are often used as a proxy to assess environmental conditions of a given area and, generally, greening is linked to an increase in vegetation productivity (i.e., better conditions) while browning indicates a reduction in productivity (i.e., degradation) (Wessels et al., 2007). However, remotely sensed measures of greening do not always imply healthier lands, as greening may also result from loss in biodiversity (e.g., monoculture plantations) or increasing concentration of invasive species (Herrmann and Tappan, 2013). For instance, reforestation of old-growth grasslands deemed suitable to offset deforestation may reduce plant and animal richness as well as carbon storage rates via changes in the surface albedo (Bond, 2016; Veldman et al., 2019). Similarly, the encroachment of woody plants is the main driver of greening trends in Africa (Brandt et al., 2017; Venter et al., 2018), yet often perceived as a degradation of ecosystems by livestock keepers as the non-palatability of encroaching species reduces the land grazing capacity (Gillson and Hoffman, 2007; Munyati et al., 2011; Sandhage-Hofmann et al., 2015). On the other hand, associating browning uniquely with land degradation would be an oversimplification, particularly from a rangeland perspective. This is because rangelands are such dynamic and heterogeneous systems, where the interactions of different disturbances (e.g., climate variability, fire regimes, herbivore pressure) may lead to different forms of land degradation (Engler and von Wehrden, 2018) or, as we show here, may be even associated with an increase in short herbaceous vegetation and hence resources. Likewise, recent local-scale studies have shown that the long-lasting presence of herders did not cause the depletion of nutrient-rich hotspots of some African savannas, but it actually enhanced their longevity over time (Marshall et al., 2018).

4.1 *Climatic vegetation cover changes*

The connection between water availability and vegetation greening in the arid and semi-arid Sahel is well-established, as shown by many studies (Anyamba and Tucker, 2005; Fensholt et al., 2009; Herrmann and Hutchinson, 2005; Hickler et al., 2005; Huber et al., 2011; Nicholson, 2005). As expected, our findings based on precipitation and soil moisture satellite data confirmed this evidence. Further, LPJ-GUESS simulations forced with precipitation, temperature, sunshine duration, nitrogen deposition, and CO_2 suggested the overall climatic behaviour of the greening Sahel. In southern Africa, trends in the different indicators were less consistent. On the one hand, the discrepancies observed within satellite and model data may reflect dynamics in shrub vegetation, which are part of the VOD and aboveground carbon signals but not captured by tree cover and woody biomass carbon signals (e.g., if large trees are removed, the tree cover signal reduces even if shrubs and bushes increase). On the other, they leave room for other interpretations embracing interactions between human and non-human forces (e.g., rainfall variability, fire, soil fertility, large mammals, rising CO_2) (Lehmann et al., 2011; Parr et al., 2014). While understanding how these factors feedback to determine the woody-herbaceous distribution remains a key and complex issue (Osborne et al., 2018), here we show that the greening of western Sahel, Chad, and southern Africa was not only associated with an increase in trees and shrubs (Brandt et al., 2016, 2015; Stevens et al., 2016; Venter et al., 2018), but also in herbaceous vegetation. One could argue that these species are often in competition (e.g., encroaching shrubs reduces the herbaceous cover), yet coexistence may still occur given the different rooting depth and temporal water use (Staver, 2018). Meanwhile, the concomitant long-term decrease in bare ground observed in these regions represents a direct data-driven clue against desert expansion claims.

4.2 *Non-climatic vegetation cover changes*

Both the greening of West Africa and South Sudan and the browning of Angola and Mozambique appeared not to be linked to changes in water availability. In addition to this, the biomass carbon simulated by LPJ-GUESS reinforced these findings and indicated that ecosystem responses to other climatic factors cannot provide an adequate explanation for the observed trends either. For instance, LPJ-GUESS was unable to reproduce the greening observed in West African rangelands principally because it was forced with climate variables that did not change significantly during 1982-2015. Similarly, in Angola the model failed to reproduce the vegetation browning observed from satellite data because precipitation (and likely the other input variables) increased between 1982 and 2015 and, in turn, simulated an increase in vegetation greenness. Ultimately, we suggest these trends to be largely driven by non-climatic forces such as herbivores, land use change, or fire, among others (not investigated in this study) (Archibald and Hempson, 2016). The vegetation structure of these rangelands (i.e., woody and short vegetation showing opposing trends) being significantly different from the climatic ones (i.e., woody and short vegetation both increasing) highlights how regional variability in the intensity and interactions of biotic and abiotic factors can produce quite different responses in vegetation growth (Osborne et al., 2018).

Non-climatic vegetation dynamics were controlled by changes in woody cover, with short vegetation having no influence on the overall greenness level. A decrease in short vegetation did not result in a decrease in greenness where woody cover increased (West Africa, South Sudan). Vice versa, vegetation browned as woody cover decreased even if the short vegetation increased (Angola, Mozambique). The West Africa and South Sudan green-up may relate to conflicts, lowering the pressure on land as people get displaced (e.g., reduced land clearance for agriculture and settlement, reduced grazing pressure) (Hugo, 1996; Olsson et al., 2005), or to other important rangeland disturbances including fire (e.g., fire suppression), or changes in wildlife and livestock numbers (Andela et al., 2017; Venter et al., 2017). However, disentangling their net effect on vegetation cover is more locally than continentally detectable (Archer et al., 2017; Devine et al., 2017). Further, recent studies showed that woody encroachment in savannas was fuelled by short-term changes in rainfall patterns (Brandt et al., 2019; Gherardi and Sala, 2015; Zhang et al., 2019), meaning that more attention should be given to the role of rainfall shifts that may not be visible in annual mean products. Short-term disturbances may indeed produce fast variations in vegetation greenness, introducing potential uncertainties in the identification of slower long-term trends (Broich et al., 2014). On the other hand, the browning of Angolan and Mozambican rangelands is likely explained by deforestation, as highlighted by the decrease in tree cover (i.e., plants $\geq$ 5 m) and previous studies (Achard et al., 2014; Cherlet et al., 2018;

Chiteculo et al., 2018; Hansen et al., 2013). Still, the latitudinal proximity of Madagascar also experiencing browning suggests that climate might have contributed, to some extent, to the final vegetation cover composition of these rangelands.

5 Implications and conclusions

The observed changes in the vegetation structure in West Africa, South Sudan, Angola, and Mozambique do not allow for a simple evaluation of greening and browning trends on the ecosystem service provision by rangelands. Although browning generally implies a reduction in the carbon uptake by terrestrial ecosystems (i.e., low climate change mitigation potential), the increase in short vegetation may hint that more herbaceous vegetation, and therefore resources, are available for pastoral communities and their livestock. On the other hand, greening trends related to woody plant encroachment increase the standing biomass, which is desirable for climate change mitigation, yet unpalatable woody species replacing short herbaceous vegetation informs of degradation of rangelands in terms of their socio-economic use. Therefore, these results suggest that future rangeland management strategies may have to balance pastoral welfare and climate change mitigation goals. Also, while the use of LPJ-GUESS corroborates the identification of climatic and non-climatic rangelands, it is worth mentioning that uncertainties in the parameterization of ecosystem processes (Zaehle et al., 2005) and in the use of large-scale climate data (Wu et al., 2017) within DGVMs contribute to uncertainties in the simulated response to climatic variability and trends, which will be particularly pronounced in the case of climatic signals with opposing impacts on simulated AGC or WDC. However, our simulation results are in many cases corroborated by the analysis of precipitation and soil moisture impacts, and agreement in the trends of simulated carbon pools and VOD provide confidence in the use of a DGVM to derive expected climate-driven trends. Finally, it is worth recalling that we considered woody shrubs to be best represented by VOD and short vegetation to mostly include herbaceous plants. Herbaceous-shrub mixing occurs at a spatial resolution undetectable from most long-term remote sensing products, and future assessments of greening and browning trends at higher spatial resolution will lift this current drawback of our study (e.g., Cheng et al., 2020; Li et al., 2020). Nonetheless, we believe that our findings still represent an important starting point for those national and local governments aiming to devise effective rangeland management strategies. This is particularly the case of rangelands in developing countries (e.g., South Sudan, Chad, Angola), where field-based rangeland assessments are often lacking due to inadequate resources and political instability.

Contributions

FD, BO, JD, and MB designed the study and methodology. FD (NDVI, VCFs, P, and SM) and MB (VOD) preprocessed the data. GS produced the LPJ-GUESS model simulations. FD, BO, and JD drafted the paper content. FD conducted the analyses, wrote the initial draft of the manuscript, and made the figures. All authors contributed to the interpretation of the findings and to the text.

Data availability

The GIMMS NDVI3g.v1 product is available in NetCDF file format at the NASA ECOCAST portal https://ecocast.arc.nasa.gov/data/pub/gimms/3g.v1/. VOD raster data and the LPJ-GUESS model outputs are available from Martin Brandt and Guy Schurgers. Vegetation continuous fields are available from the USGS LP DAAC catalogue https://lpdaac.usgs.gov/products/vcf5kyrv001/. The NetCDF monthly CHIRPS precipitation dataset is available from the Climate Hazard Group, UC Santa Barbara (ftp://ftp.chg.ucsb.edu/pub/org/chg/products/CHIRPS-2.0). The ESA CCI soil moisture product can be obtained at http://www.esa-soilmoisture-cci.org/node/145. The MODIS MCD12C1 land cover product collection 6 was accessed and downloaded via Google Earth Engine (https://code.earthengine.google.com). The Ellis et al. (2010) anthropogenic biome classification is available at http://ecotope.org/anthromes/v2/data/. The UNESCO White (1983) Vegetation of Africa map is available from the UNEP Environmental Data Explorer (https://ede.grid.unep.ch/). The aridity index map is available from the FAO (http://ref.data.fao.org/map?entryId=f8cf2780-88fd-11da-a88f-000d939bc5d8).

Declaration of competing interest

The authors declare no conflicting interests.

Acknowledgements

We thank all research groups that produced and shared the datasets used in this study. We thank JP Guzman for the support with R Studio; F Detsch for addressing the use of the CRAN package 'gimms'; J Sheffield for the suggestions on quality controls; LA Brown, C Abel, R Fensholt, and S Horion for the discussions. FD was partly funded by the European Cooperation in Science and Technology (COST) Action CA16233 'Drylands facing change: interdisciplinary research on climate change, food insecurity, political instability'. MB was funded by an AXA research grant and a DFF Sapere Aude grant.

References

Abel, C., Horion, S., Tagesson, T., Brandt, M., Fensholt, R., 2019. Towards improved remote sensing based monitoring of dryland ecosystem functioning using sequential linear regression slopes (SeRGS). Remote Sens. Environ. 224, 317–332. doi:10.1016/j.rse.2019.02.010

Achard, F., Beuchle, R., Mayaux, P., Stibig, H.J., Bodart, C., Brink, A., Carboni, S., Desclée, B., Donnay, F., Eva, H.D., Lupi, A., Raši, R., Seliger, R., Simonetti, D., 2014. Determination of tropical deforestation rates and related carbon losses from 1990 to 2010. Glob. Chang. Biol. 20, 2540–2554. doi:10.1111/gcb.12605

Ahlström, A., Raupach, M.R., Schurgers, G., Smith, B., Arneth, A., Jung, M., Reichstein, M., Canadell, J.P., Friedlingstein, P., Jain, A.K., Kato, E., Poulter, B., Sitch, S., Stocker, B.D., Viovy, N., Wang, Y.P., Wiltshire, A., Zaehle, S., Zeng, N., 2015. The dominant role of semi-arid ecosystems in the trend and variability of the land CO2 sink. Science. 348, 895–899. doi:10.1002/2015JA021022

Alkemade, R., Reid, R.S., van den Berg, M., de Leeuw, J., Jeuken, M., 2013. Assessing the impacts of livestock production on biodiversity in rangeland ecosystems. Proc. Natl. Acad. Sci. 110, 20900–20905. doi:10.1073/pnas.1011013108

Allen, V.G., Batello, C., Berretta, E.J., Hodgson, J., Kothmann, M., Li, X., McIvor, J., Milne, J., Morris, C., Peeters, A., Sanderson, M., 2011. An international terminology for grazing lands and grazing animals.

Grass Forage Sci. 66, 2–28. doi:10.1111/j.1365-2494.2010.00780.x

Andela, N., Liu, Y.Y., M. Van Dijk, A.I.J., De Jeu, R.A.M., McVicar, T.R., 2013. Global changes in dryland vegetation dynamics (1988-2008) assessed by satellite remote sensing: Comparing a new passive microwave vegetation density record with reflective greenness data. Biogeosciences 10, 6657–6676. doi:10.5194/bg-10-6657-2013

Andela, N., Morton, D.C., Giglio, L., Chen, Y., Van Der Werf, G.R., Kasibhatla, P.S., DeFries, R.S., Collatz, G.J., Hantson, S., Kloster, S., Bachelet, D., Forrest, M., Lasslop, G., Li, F., Mangeon, S., Melton, J.R., Yue, C., Randerson, J.T., 2017. A human-driven decline in global burned area. Science. 356, 1356–1362. doi:10.1126/science.aal4108

Anyamba, A., Small, J.L., Tucker, C.J., Pak, E.W., 2014. Thirty-two Years of Sahelian Zone Growing Season Non-Stationary NDVI3g Patterns. Remote Sens. 6, 3101–3122. doi:10.3390/rs6043101

Anyamba, A., Tucker, C.J., 2005. Analysis of Sahelian vegetation dynamics using NOAA-AVHRR NDVI data from 1981-2003. J. Arid Environ. 63, 596–614. doi:10.1016/j.jaridenv.2005.03.007

Archer, S.R., Andersen, E.M., Predick, K.I., Schwinning, S., Steidl, R.J., Woods, S.R., 2017. Woody Plant Encroachment: Causes and Consequences, in: Briske, D.D. (Ed.), Rangeland Systems. Springer, Cham, Switzerland, pp. 25–84. doi:10.1007/978-3-319-46709-2

Archibald, S., Hempson, G.P., 2016. Competing consumers: Contrasting the patterns and impacts of fire and mammalian herbivory in Africa: Supplementary. Philos. Trans. R. Soc. B Biol. Sci. 371. doi:10.1098/rstb.2015.0309

Axelsson, C.R., Hanan, N.P., 2018. Rates of woody encroachment in African savannas reflect water constraints and fire disturbance. J. Biogeogr. 45, 1209–1218. doi:10.1111/jbi.13221

Bao, G., Bao, Y., Sanjjava, A., Qin, Z., Zhou, Y., Xu, G., 2015. NDVI-indicated long-term vegetation dynamics in Mongolia and their response to climate change at biome scale. Int. J. Climatol. 35, 4293–4306. doi:10.1002/joc.4286

Benayas, J.M.R., Martins, A., Nicolau, J.M., Schulz, J.J., 2007. Abandonment of agricultural land: An overview of drivers and consequences. CAB Rev. Perspect. Agric. Vet. Sci. Nutr. Nat. Resour. 2. doi:10.1079/PAVSNNR20072057

Bi, J., Xu, L., Samanta, A., Zhu, Z., Myneni, R., 2013. Divergent Arctic-Boreal vegetation changes between North America and Eurasia over the past 30 years. Remote Sens. 5, 2093–2112. doi:10.3390/rs5052093

Bond, W., Zaloumis, N.P., 2016. The deforestation story: Testing for anthropogenic origins of Africa's flammable grassy biomes. Philos. Trans. R. Soc. B Biol. Sci. 371: 20150. doi:10.1098/rstb.2015.0170

Bond, W.J., 2016. Ancient grasslands at risk. Science. 351, 120–122. doi:10.1126/science.aad5132

Bond, W.J., Woodward, F.I., Midgley, G.F., 2005. The global distribution of ecosystems in a world without fire. New Phytol. 165, 525–538. doi:10.1111/j.1469-8137.2004.01252.x

Brandt, M., Hiernaux, P., Rasmussen, K., Tucker, C.J., Wigneron, J.-P., Diouf, A.A., Herrmann, S.M., Zhang, W., Kergoat, L., Mbow, C., Abel, C., Auda, Y., Fensholt, R., 2019. Changes in rainfall distribution promote woody foliage production in the Sahel. Commun. Biol. 2, 133. doi:10.1038/s42003-019-0383-9

Brandt, M., Hiernaux, P., Tagesson, T., Verger, A., Rasmussen, K., Diouf, A.A., Mbow, C., Mougin, E., Fensholt, R., 2016. Woody plant cover estimation in drylands from Earth Observation based seasonal metrics. Remote Sens. Environ. 172, 28–38. doi:10.1016/j.rse.2015.10.036

Brandt, M., Mbow, C., Diouf, A.A., Verger, A., 2015. Ground- and satellite-based evidence of the biophysical mechanisms behind the greening Sahel. Glob. Chang. Biol. 1610–1620. doi:10.1111/gcb.12807

Brandt, M., Rasmussen, K., Peñuelas, J., Tian, F., Schurgers, G., Verger, A., Mertz, O., Palmer, J.R.B., Fensholt, R., 2017. Human population growth offsets climate-driven increase in woody vegetation in sub-Saharan Africa. Nat. Ecol. Evol. 1, 0081. doi:10.1038/s41559-017-0081

Brandt, M., Tucker, C.J., Kariryaa, A., Rasmussen, K., Abel, C., Small, J., Chave, J., Rasmussen, L.V., Hiernaux, P., Diouf, A.A., Kergoat, L., Mertz, O., Igel, C., Gieseke, F., Schöning, J., Li, S., Melocik, K., Meyer, J., Sinno, S., Romero, E., Glennie, E., Montagu, A., Dendoncker, M., Fensholt, R., 2020. An unexpectedly large count of trees in the West African Sahara and Sahel. Nature 587. doi:10.1038/s41586-020-2824-5

Brandt, M., Wigneron, J.P., Chave, J., Tagesson, T., Penuelas, J., Ciais, P., Rasmussen, K., Tian, F., Mbow, C., Al-Yaari, A., Rodriguez-Fernandez, N., Schurgers, G., Zhang, W., Chang, J., Kerr, Y., Verger, A., Tucker, C., Mialon, A., Rasmussen, L.V., Fan, L., Fensholt, R., 2018. Satellite passive microwaves reveal recent climate-induced carbon losses in African drylands. Nat. Ecol. Evol. 2, 827–835. doi:https://doi.org/10.1038/s41559-018-0530-6

Broich, M., Huete, A., Tulbure, M.G., Ma, X., Xin, Q., Paget, M., Restrepo-Coupe, N., Davies, K., Devadas, R., Held, A., 2014. Land surface phenological response to decadal climate variability across Australia using satellite remote sensing. Biogeosciences 11, 5181–5198. doi:10.5194/bg-11-5181-2014

Bromley, L., 2010. Relating violence to MODIS fire detections in. Int. J. Remote Sens. 31:9, 2277–2292. doi:10.1080/01431160902953909

Burrell, A.L., Evans, J.P., Liu, Y., 2018. The impact of dataset selection on land degradation assessment. ISPRS J. Photogramm. Remote Sens. 146, 22–37. doi:10.1016/j.isprsjprs.2018.08.017

Cheng, Y., Vrieling, A., Fava, F., Meroni, M., Marshall, M., Gachoki, S., 2020. Phenology of short vegetation cycles in a Kenyan rangeland from PlanetScope and Sentinel-2. Remote Sens. Environ. 248, 112004. doi:10.1016/j.rse.2020.112004

Cherlet, M., Hutchinson, C., Reynolds, J., Hill, J., Sommer, S., von Maltitz, G. (Eds.), World Atlas of Desertification, Publication Office of the European Union, Luxembourg, 2018

Chiteculo, V., Abdollahnejad, A., Panagiotidis, D., Surový, P., Sharma, R.P., 2018. Defining deforestation patterns using satellite images from 2000 and 2017: Assessment of forest management in Miombo forests-A case study of Huambo province in Angola. Sustain. 11. doi:10.3390/su11010098

Chung, D., Dorigo, W., De Jeu, R., Kidd, R., Wagner, W., 2018a. Product Specification Document (PSD) Version 4.2. ESA Bulletin

Chung, D., Dorigo, W., Hahn., S., Melzer., T., Paulik., C., Reimer, C., Vreugdenhil, M., Wagner, W., Kidd, R., 2018b. Algorithm Theoretical Baseline Document (ATBD) Merging Active and Passive Soil Moisture Retrievals. ESA Bulletin

Daskin, J.H., Stalmans, M., Pringle, R.M., 2016. Ecological legacies of civil war: 35-year increase in savanna tree cover following wholesale large-mammal declines. J. Ecol. 104, 79–89. doi:10.1111/1365-2745.12483

Detsch, F., 2016. Download and Process GIMMS NDVI3g Data. R CRAN Project

Devine, A.P., McDonald, R.A., Quaife, T., Maclean, I.M.D., 2017. Determinants of woody encroachment and cover in African savannas. Oecologia 183, 939–951. doi:10.1007/s00442-017-3807-6

Dixon, J., Gulliver, A., Gibbon, D., 2001. Farming Systems and Poverty: Improving Farmers' Livelihoods in a Changing World. Rome & Washington

Dobson, M., Borner, A., Sinclair, T., 2010. Road will ruin Serengeti. Nature 467, 272–273. doi:10.1038/467272a

Dorigo, W., Wagner, W., Albergel, C., Albrecht, F., Balsamo, G., Brocca, L., Chung, D., Ertl, M., Forkel, M., Gruber, A., Haas, E., Hamer, P.D., Hirschi, M., Ikonen, J., de Jeu, R., Kidd, R., Lahoz, W., Liu, Y.Y., Miralles, D., Mistelbauer, T., Nicolai-Shaw, N., Parinussa, R., Pratola, C., Reimer, C., van der Schalie, R., Seneviratne, S.I., Smolander, T., Lecomte, P., 2017. ESA CCI Soil Moisture for improved Earth system understanding: State-of-the art and future directions. Remote Sens. Environ. 203, 185–215. doi:10.1016/j.rse.2017.07.001

Dorigo, W.A., Gruber, A., De Jeu, R.A.M., Wagner, W., Stacke, T., Loew, A., Albergel, C., Brocca, L., Chung, D., Parinussa, R.M., Kidd, R., 2015. Evaluation of the ESA CCI soil moisture product using ground-based observations. Remote Sens. Environ. 162, 380–395. doi:10.1016/j.rse.2014.07.023

Dorigo, W.A., Scipal, K., Parinussa, R.M., Liu, Y.Y., Wagner, W., De Jeu, R.A.M., Naeimi, V., 2010. Error characterisation of global active and passive microwave soil moisture datasets. Hydrol. Earth Syst. Sci.

14, 2605–2616. doi:10.5194/hess-14-2605-2010

Eastman, J.R., Sangermano, F., Machado, E.A., Rogan, J., Anyamba, A., 2013. Global trends in seasonality of Normalized Difference Vegetation Index (NDVI), 1982-2011. Remote Sens. 5, 4799–4818. doi:10.3390/rs5104799

Ellis, E.C., Goldewijk, K.K., Siebert, S., Lightman, D., Ramankutty, N., 2010. Anthropogenic transformation of the biomes, 1700 to 2000. Glob. Ecol. Biogeogr. 19, 589–606. doi:10.1111/j.1466-8238.2010.00540.x

Elvidge, C.D., Lyon, R.J.P., 1985. Influence of rock-soil spectral variation on the assessment of green biomass. Remote Sens. Environ. 17, 265–279. doi:10.1016/0034-4257(85)90099-9

Engler, J.O., von Wehrden, H., 2018. Global assessment of the non-equilibrium theory of rangelands: Revisited and refined. Land use policy 70, 479–484. doi:10.1016/j.landusepol.2017.11.026

Etheridge, D.M., Steele, L.P., Langenfelds, R.L., Francey, R.J., Barnola, J.M., Morgan, V.I., 1996. Natural and anthropogenic changes in atmospheric CO2 over the last 1000 years from air in Antarctic ice and firn. J. Geophys. Res. Atmos. 101, 4115–4128. doi:10.1029/95JD03410

FAO, 2017. Sustainable Pastoralism and Rangelands in Africa. Accra

Fensholt, R., Langanke, T., Rasmussen, K., Reenberg, A., Prince, S.D., Tucker, C., Scholes, R.J., Le, Q.B., Bondeau, A., Eastman, R., Epstein, H., Gaughan, A.E., Hellden, U., Mbow, C., Olsson, L., Paruelo, J., Schweitzer, C., Seaquist, J., Wessels, K., 2012. Greenness in semi-arid areas across the globe 1981-2007 - an Earth Observing Satellite based analysis of trends and drivers. Remote Sens. Environ. 121, 144–158. doi:10.1016/j.rse.2012.01.017

Fensholt, R., Rasmussen, K., Nielsen, T.T., Mbow, C., 2009. Evaluation of earth observation based long term vegetation trends - Intercomparing NDVI time series trend analysis consistency of Sahel from AVHRR GIMMS, Terra MODIS and SPOT VGT data. Remote Sens. Environ. 113, 1886–1898. doi:10.1016/j.rse.2009.04.004

Flintan, F., 2012. Making rangelands secure: past experience and future options, International Land Coalition

(ILC), Rome

Forkel, M., Carvalhais, N., Verbesselt, J., Mahecha, M.D., Neigh, C.S.R., Reichstein, M., 2013. Trend Change detection in NDVI time series: Effects of inter-annual variability and methodology. Remote Sens. 5, 2113–2144. doi:10.3390/rs5052113

Funk, C., Peterson, P., Landsfeld, M., Pedreros, D., Verdin, J., Shukla, S., Husak, G., Rowland, J., Harrison, L., Hoell, A., Michaelsen, J., 2015. The climate hazards infrared precipitation with stations—a new environmental record for monitoring extremes. Sci. Data 2, 150066. doi:10.1038/sdata.2015.66

Funk, C.C., Peterson, P.J., Landsfeld, M.F., Pedreros, D.H., Verdin, J.P., Rowland, J.D., Romero, B.E., Husak, G.J., Michaelsen, J.C., Verdin, A.P., 2014. A Quasi-Global Precipitation Time Series for Drought Monitoring. U.S. Geol. Surv. Data Ser. 832, 4. doi:http://dx.doi.org/110.3133/ds832

Gherardi, L.A., Sala, O.E., 2015. Enhanced precipitation variability decreases grass- and increases shrub-productivity. Proc. Natl. Acad. Sci. 112, 12735–12740. doi:10.1073/pnas.1506433112

Gillson, L., Hoffman, M.T., 2007. Rangeland ecology in a changing world. Science. 315, 53–54. doi:10.1126/science.1136577

Gizaw, M.S., Gan, T.Y., 2017. Impact of climate change and El Niño episodes on droughts in sub-Saharan Africa. Clim. Dyn. 49, 665–682. doi:10.1007/s00382-016-3366-2

Gorsevski, V., Kasischke, E., Dempewolf, J., Loboda, T., Grossmann, F., 2012. Analysis of the Impacts of armed conflict on the Eastern Afromontane forest region on the South Sudan - Uganda border using multitemporal Landsat imagery. Remote Sens. Environ. 118, 10–20. doi:10.1016/j.rse.2011.10.023

Gruber, A., Scanlon, T., van der Schalie, R., Wagner, W., Dorigo, W., 2019. Evolution of the ESA CCI Soil Moisture climate data records and their underlying merging methodology. Earth Syst. Sci. Data 11, 717–739. doi:10.5194/essd-11-717-2019

Hansen, M.C., Potapov, P. V., Moore, R., Hancher, M., Turubanova, S.A., Tyukavina, A., Thau, D., Stehman, S. V., Goetz, S.J., Loveland, T.R., Kommareddy, A., Egorov, A., Chini, L., Justice, C.O., Townshend, J.R.G., 2013. High-Resolution Global Maps of 21st-Century Forest Cover Change. Science. 342, 850–853. doi:10.1126/science.1244693

Harris, I., Jones, P.D., Osborn, T.J., Lister, D.H., 2014. Updated high-resolution grids of monthly climatic observations - the CRU TS3.10 Dataset. Int. J. Climatol. 34, 623–642. doi:10.1002/joc.3711

Helldén, U., Tottrup, C., 2008. Regional desertification: A global synthesis. Glob. Planet. Change 64, 169–176. doi:10.1016/j.gloplacha.2008.10.006

Herrmann, S.M., Anyamba, A., Tucker, C.J., 2005. Recent trends in vegetation dynamics in the African Sahel and their relationship to climate. Glob. Environ. Chang. 15, 394–404. doi:10.1016/j.gloenvcha.2005.08.004

Herrmann, S.M., Hutchinson, C.F., 2005. The changing contexts of the desertification debate. J. Arid Environ. 63, 538–555. doi:10.1016/j.jaridenv.2005.03.003

Herrmann, S.M., Tappan, G.G., 2013. Vegetation impoverishment despite greening: A case study from central Senegal. J. Arid Environ. 90, 55–66. doi:10.1016/j.jaridenv.2012.10.020

Hickler, T., Eklundh, L., Seaquist, J.W., Smith, B., Ardö, J., Olsson, L., Sykes, M.T., Sjöström, M., 2005. Precipitation controls Sahel greening trend. Geophys. Res. Lett. 32, 1–4. doi:10.1029/2005GL024370

Hijmans, R.J., van Etter, J., Sumner, M., Cheng, J., Baston, Bevan, A., Bivand, R., Busetto, L., Canty, M., Fasoli, B., Forrest, D., Ghosh, A., Golicher, D., Gray, J., M., Greenberg, J.A., Hiemstra, P., Hingee, K., Karney, C., Mattiuzzi, Mosher, S., Naimi, B., Nowosad, J., Pebesma, E., Lamigueiro, O.P., Racine, E.B., Rowlingson, B., Shortridge, A., Vanables, B., ueest, R., 2021. Geographic Data Analysis and Modeling. R CRAN Project

Hirota, M., Holmgren, M., van Nes, E.H., Scheffer, M., 2011. Global Resilience of Tropical Forest. Science. 334, 232–235

Hobbs, N.T., Galvin, K.A., Stokes, C.J., Lackett, J.M., Ash, A.J., Boone, R.B., Reid, R.S., Thornton, P.K., 2008. Fragmentation of rangelands: Implications for humans, animals, and landscapes. Glob. Environ.

Chang. 18, 776–785. doi:10.1016/j.gloenvcha.2008.07.011

Hoffman, T., Vogel, C., 2008. Climate change impacts on African Rangeland. Rangelands 30, 12–17. doi:http://dx.doi.org/10.2111/1551-501X(2008)30[12:CCIOAR]2.0.CO;2

Hoscilo, A., Balzter, H., Bartholomé, E., Boschetti, M., Brivio, P.A., Brink, A., Clerici, M., 2015. A conceptual model for assessing rainfall and vegetation trends in sub-Saharan Africa from satellite data. Int. J. Climatol. 3592, 3582–3592. doi:10.1002/joc.4231

Huber, S., Fensholt, R., Rasmussen, K., 2011. Water availability as the driver of vegetation dynamics in the African Sahel from 1982 to 2007. Glob. Planet. Change 76, 186–195. doi:10.1016/j.gloplacha.2011.01.006

Huete, A.R., 1988. A soil-adjusted vegetation index (SAVI). Remote Sens. Environ. 25, 295–309. doi:10.1016/0034-4257(88)90106-X

Hugo, G., 1996. Environmental Concerns and International Migration. Environ. Concerns Int. Migr. 30, 105–131. doi:10.1080/08882746.1997.11430277

Ibrahim, Y.Z., Balzter, H., Kaduk, J., Tucker, C.J., 2015. Land degradation assessment using residual trend analysis of GIMMS NDVI3g, soil moisture and rainfall in Sub-Saharan West Africa from 1982 to 2012. Remote Sens. 7, 5471–5494. doi:10.3390/rs70505471

Kharin, V. V., Zwiers, F.W., Zhang, X., Hegerl, G.C., 2007. Changes in temperature and precipitation extremes in the IPCC ensemble of global coupled model simulations. J. Clim. 20, 1419–1444. doi:10.1175/JCLI4066.1

Kiage, L.M., 2013. Perspectives on the assumed causes of land degradation in the rangelands of Sub-Saharan Africa. Prog. Phys. Geogr. 37, 664–684. doi:10.1177/0309133313492543

Lal, R., 2004. Soil Carbon Sequestration Impacts on Global Climate Change and Food Security. Science. 304, 1623–1627. doi:10.1126/science.1097396

Lamarque, J.F., Dentener, F., McConnell, J., Ro, C.U., Shaw, M., Vet, R., Bergmann, D., Cameron-Smith, P., Dalsoren, S., Doherty, R., Faluvegi, G., Ghan, S.J., Josse, B., Lee, Y.H., Mackenzie, I.A., Plummer, D., Shindell, D.T., Skeie, R.B., Stevenson, D.S., Strode, S., Zeng, G., Curran, M., Dahl-Jensen, D., Das, S., Fritzsche, D., Nolan, M., 2013. Multi-model mean nitrogen and sulfur deposition from the atmospheric chemistry and climate model intercomparison project (ACCMIP): Evaluation of historical and projected future changes. Atmos. Chem. Phys. 13, 7997–8018. doi:10.5194/acp-13-7997-2013

Lange, M., Eisenhauer, N., Sierra, C.A., Bessler, H., Engels, C., Griffiths, R.I., Mellado-Vázquez, P.G., Malik, A.A., Roy, J., Scheu, S., Steinbeiss, S., Thomson, B.C., Trumbore, S.E., Gleixner, G., 2015. Plant diversity increases soil microbial activity and soil carbon storage. Nat. Commun. 6. doi:10.1038/ncomms7707

Lehmann, C.E.R., Archibald, S.A., Hoffmann, W.A., Bond, W.J., 2011. Deciphering the distribution of the savanna biome. New Phytol. 191, 197–209. doi:10.1111/j.1469-8137.2011.03689.x

Lehsten, V., Tansey, K., Balzter, H., Thonicke, K., Spessa, A., Weber, U., Smith, B., Arneth, A., 2009. Estimating carbon emissions from African wildfires. Biogeosciences 6, 349–360. doi:10.5194/bg-6-349-2009

Li, W., Buitenwerf, R., Munk, M., Bøcher, P.K., Svenning, J.C., 2020. Deep-learning based high-resolution mapping shows woody vegetation densification in greater Maasai Mara ecosystem. Remote Sens. Environ. 247, 111953. doi:10.1016/j.rse.2020.111953

Liu, Y.Y., De Jeu, R.A.M., McCabe, M.F., Evans, J.P., Van Dijk, A.I.J.M., 2011. Global long-term passive microwave satellite-based retrievals of vegetation optical depth. Geophys. Res. Lett. 38, 1–6. doi:10.1029/2011GL048684

Liu, Y.Y., van Dijk, A.I.J.M., de Jeu, R. a M., Canadell, J.G., McCabe, M.F., Evans, J.P., Wang, G., 2015. Recent reversal in loss of global terrestrial biomass. Nat. Clim. Chang. 5, 1–5. doi:10.1038/nclimate2581

Lund, H.G., 2007. Accounting for the World's Rangelands. Rangeland 29, 3–10. doi:DOI:10.2458/azu_rangelands_v29i1_lund

Marshall, F., Reid, R.E.B., Goldstein, S., Storozum, M., Wreschnig, A., Hu, L., Kiura, P., Shahack-Gross, R., Ambrose, S.H., 2018. Ancient herders enriched and restructured African grasslands. Nature 561, 387–390. doi:10.1038/s41586-018-0456-9

Mayer, A.L., Khalyani, A.H., 2011. Grass trumps trees with fire. Science. 334, 188–189. doi:10.1126/science.1213908

McNally, A., Husak, G.J., Brown, M., Carroll, M., Funk, C., Yatheendradas, S., Arsenault, K., Peters-Lidard, C., Verdin, J.P., 2015. Calculating Crop Water Requirement Satisfaction in the West Africa Sahel with Remotely Sensed Soil Moisture. J. Hydrometeorol. 16, 295–305. doi:10.1175/JHM-D-14-0049.1

Meesters, A.G.C.A., De Jeu, R.A.M., Owe, M., 2005. Analytical derivation of the vegetation optical depth from the microwave polarization difference index. IEEE Geosci. Remote Sens. Lett. 2, 121–123. doi:10.1109/LGRS.2005.843983

Midgley, G.F., Bond, W.J., 2015. Future of African terrestrial biodiversity and ecosystems under anthropogenic climate change. Nat. Clim. Chang. 5, 823–829. doi:10.1038/nclimate2753

Moncrieff, G.R., Bond, W.J., Higgins, S.I., 2016. Revising the biome concept for understanding and predicting global change impacts. J. Biogeogr. 43, 863–873. doi:10.1111/jbi.12701

Mueller, T., Dressler, G., Tucker, C.J., Pinzon, J.E., Leimgruber, P., Dubayah, R.O., Hurtt, G.C., Böhning-Gaese, K., Fagan, W.F., Tucker, J.C., Pinzon, E.J., Leimgruber, P., Dubayah, O.R., Hurtt, C.G., Böhning-Gaese, K., Fagan, F.W., 2014. Human Land-Use Practices Lead to Global Long-Term Increases in Photosynthetic Capacity. Remote Sens. 6, 5717–5731. doi:10.3390/rs6065717

Munyati, C., Shaker, P., Phasha, M.G., 2011. Using remotely sensed imagery to monitor savanna rangeland deterioration through woody plant proliferation: A case study from communal and biodiversity conservation rangeland sites in Mokopane, South Africa. Environ. Monit. Assess. 176, 293–311. doi:10.1007/s10661-010-1583-4

Nemani, R.R., Keeling, C.D., Tucker, C.J., Myneni, R.B., Running, S.W., 2003. Climate-Driven Increases in

Global Terrestrial Net Primary Production from 1982 to 1999. Science. 300, 1560–1563. doi:10.1126/science.1082750

Niang, I., Ruppel, O.C., Abdrabo, M.A., Essel, A., Lennard, C., Padgham, J., Urquhart, P., 2014: Africa. In: Climate Change 2014: Impacts, Adaptation, and Vulnerability. Part B: Regional Aspects. Contribution of Working Group II to the Fifth Assessment Report of the Intergovernmental Panel on Climate Change [Barros, V.R., C.B. Field, D.J. Dokken, M.D. Mastrandrea, K.J. Mach, T.E. Bilir, M. Chatterjee, K.L. Ebi, Y.O. Estrada, R.C. Genova, B. Girma, E.S. Kissel, A.N. Levy, S. MacCracken, P.R. Mastrandrea, and L.L. White (eds.)]. Cambridge University Press, Cambridge, United Kingdom and New York, NY, USA, pp. 1199-1265

Nicholson, S., 2005. On the question of the "recovery" of the rains in the West African Sahel. J. Arid Environ. 63, 615–641. doi:10.1016/j.jaridenv.2005.03.004

Nicholson, S.E., 2016. An analysis of recent rainfall conditions in eastern Africa. Int. J. Climatol. 36, 526–532. doi:10.1002/joc.4358

Oliveras, I., Malhi, Y., 2016. Many shades of green: The dynamic tropical forest–savannah transition zones. Philos. Trans. R. Soc. B Biol. Sci. 371: 20150. doi:10.1098/rstb.2015.0308

Olsson, L., Eklundh, L., Ardö, J., 2005. A recent greening of the Sahel - Trends, patterns and potential causes. J. Arid Environ. 63, 556–566. doi:10.1016/j.jaridenv.2005.03.008

Osborne, C.P., Charles-Dominique, T., Stevens, N., Bond, W.J., Midgley, G., Lehmann, C.E.R., 2018. Human impacts in African savannas are mediated by plant functional traits. New Phytol. 220, 10–24. doi:10.1111/nph.15236

Owe, M., de Jeu, R., Holmes, T., 2008. Multisensor historical climatology of satellite-derived global land surface moisture. J. Geophys. Res. Earth Surf. 113, 1–17. doi:10.1029/2007JF000769

Owe, M., De Jeu, R., Walker, J., 2001. A methodology for surface soil moisture and vegetation optical depth retrieval using the microwave polarization difference index. IEEE Trans. Geosci. Remote Sens. 39, 1643–1654. doi:10.1109/36.942542

Papagiannopoulou, C., Miralles, D.G., Dorigo, W.A., Verhoest, N.E.C., Depoorter, M., Waegeman, W., 2017. Vegetation anomalies caused by antecedent precipitation in most of the world. Environ. Res. Lett. 12, 074016. doi:10.1088/1748-9326/aa7145

Parr, C.L., Lehmann, C.E.R., Bond, W.J., Hoffmann, W.A., Andersen, A.N., 2014. Tropical grassy biomes: Misunderstood, neglected, and under threat. Trends Ecol. Evol. 29, 205–213. doi:10.1016/j.tree.2014.02.004

Pausas, J.G., Bond, W.J., 2020. Alternative Biome States in Terrestrial Ecosystems. Trends Plant Sci. 25, 250–263. doi:10.1016/j.tplants.2019.11.003

Pengra, B., Long, J., Dahal, D., Stehman, S. V., Loveland, T.R., 2015. A global reference database from very high resolution commercial satellite data and methodology for application to Landsat derived 30m continuous field tree cover data. Remote Sens. Environ. 165, 234–248. doi:10.1016/j.rse.2015.01.018

Phelps, L.N., Kaplan, J.O., 2017. Land use for animal production in global change studies: Defining and characterizing a framework. Glob. Chang. Biol. 23, 4457–4471. doi:10.1111/gcb.13732

Piao, S., Sitch, S., Ciais, P., Friedlingstein, P., Peylin, P., Wang, X., Ahlström, A., Anav, A., Canadell, J.G., Cong, N., Huntingford, C., Jung, M., Levis, S., Levy, P.E., Li, J., Lin, X., Lomas, M.R., Lu, M., Luo, Y., Ma, Y., Myneni, R.B., Poulter, B., Sun, Z., Wang, T., Viovy, N., Zaehle, S., Zeng, N., 2013. Evaluation of terrestrial carbon cycle models for their response to climate variability and to CO2 trends. Glob. Chang. Biol. 19, 2117–2132. doi:10.1111/gcb.12187

Pinzon, J.E., Tucker, C.J., 2014. A non-stationary 1981-2012 AVHRR NDVI3g time series. Remote Sens. 6, 6929–6960. doi:10.3390/rs6086929

R Core Team, 2018. R: A language and environment for statistical computing. R Foundation for Statistical Computing, Vienna, Austria, http://www.R-project.org/

Reeves, M.C., Washington-Allen, R.A., Angerer, J., Hunt, E.R., Kulawardhana, R.W., Kumar, L., Loboda, T., Loveland, T., Metternicht, G., Ramsey, R.D., 2015. Global View of Remote Sensing of Rangelands: Evolution, Applications, Future Pathways, in: Land Resources Monitoring Modeling and Mapping with Remote Sensing. Boca Raton, Florida, pp. 237–275. doi:https://doi.org/10.1201/b19322

Sala, O.E., Yahdjian, L., Havstad, K., Aguiar, M.R., 2017. Rangeland Ecosystem Services: Nature's Supply and Humans' Demand, in: Briske, D.D. (Ed.), Rangeland Systems. Springer, Cham, Switzerland, pp. 467–489. doi:10.1007/978-3-319-46709-2_14

Sallaba, F., Olin, S., Engström, K., Abdi, A.M., Boke-Olén, N., Lehsten, V., Ardö, J., Seaquist, J.W., 2017. Future supply and demand of net primary production in the Sahel. Earth Syst. Dyn. 8, 1191–1221. doi:10.5194/esd-8-1191-2017

Sandhage-Hofmann, A., Kotzé, E., van Delden, L., Dominiak, M., Fouché, H.J., van der Westhuizen, H.C., Oomen, R.J., du Preez, C.C., Amelung, W., 2015. Rangeland management effects on soil properties in the savanna biome, South Africa: A case study along grazing gradients in communal and commercial farms. J. Arid Environ. 120, 14–25. doi:10.1016/j.jaridenv.2015.04.004

Sankaran, M., Hanan, N.P., Scholes, R.J., Ratnam, J., Augustine, D.J., Cade, B.S., Gignoux, J., Higgins, S.I., Le Roux, X., Ludwig, F., Ardo, J., Banyikwa, F., Bronn, A., Bucini, G., Caylor, K.K., Coughenour, M.B., Diouf, A., Ekaya, W., Feral, C.J., February, E.C., Frost, P.G.H., Hiernaux, P., Hrabar, H., Metzger, K.L., Prins, H.H.T., Ringrose, S., Sea, W., Tews, J., Worden, J., Zambatis, N., 2005. Determinants of woody cover in African savannas. Nature 438, 846–849. doi:10.1038/nature04070

Sayre, N.F., Davis, D.K., Bestelmeyer, B., Williamson, J.C., 2017. Rangelands: Where Anthromes Meet Their Limits. Land 6, 31. doi:10.3390/land6020031

Schurgers, G., Ahlström, A., Arneth, A., Pugh, T.A.M., Smith, B., 2018. Climate Sensitivity Controls Uncertainty in Future Terrestrial Carbon Sink. Geophys. Res. Lett. 45, 4329–4336. doi:10.1029/2018GL077528

Sitch, S., Smith, B., I.A., P., Arneth, A., Bondeau, A., Cramer, W., Kaplan, J.O., Levis, S., Lucht, W., Sykes, M.T., Thonicke, K., Venevsky, S., 2003. Evaluation of ecosystem dynamics, plant geography and terrestrial carbon cycling in the LPJ dynamic global vegetation model. Glob. Chang. Biol. 9, 161–185. doi:10.1097/01.HJ.0000348529.60214.24

Skowno, A.L., Thompson, M.W., Hiestermann, J., Ripley, B., West, A.G., Bond, W.J., 2017. Woodland expansion in South African grassy biomes based on satellite observations (1990–2013): general patterns and potential drivers. Glob. Chang. Biol. 23, 2358–2369. doi:10.1111/gcb.13529

Smith, B., Prentice, I.C., Sykes, M.T., 2001. Representation of vegetation dynamics in the modelling of terrestrial ecosystems: Comparing two contrasting approaches within European climate space. Glob. Ecol. Biogeogr. 10, 621–637. doi:10.1046/j.1466-822X.2001.00256.x

Smith, B., Wärlind, D., Arneth, A., Hickler, T., Leadley, P., Siltberg, J., Zaehle, S., 2014. Implications of incorporating N cycling and N limitations on primary production in an individual-based dynamic vegetation model. Biogeosciences 11, 2027–2054. doi:10.5194/bg-11-2027-2014

Song, X.-P., Hansen, M.C., Stehman, S. V., Potapov, P. V., Tyukavina, A., Vermote, E.F., Townshend, J.R., 2018. Global land change from 1982 to 2016. Nature 560, 639–643. doi:10.1038/s41586-018-0411-9

Song, X., DiMiceli, C., Carroll, M., Sohlberg, R., Kim, D.-H., Townshend, J., 2018. MEaSURES Vegetation Continuous Fields ESDR Algorithm Theoretical Basis Document (ATBD). University of Maryland, College Park

Staver, A.C., 2018. Prediction and scale in savanna ecosystems. New Phytol. 219, 52–57. doi:10.1111/nph.14829

Staver, A.C., Archibald, S., Levin, S.A., 2011. The global extent and determinants of savanna and forest as alternative biome states. Science. 334, 230–232. doi:10.1126/science.1210465

Stevens, N., Erasmus, B.F.N., Archibald, S., Bond, W.J., 2016. Woody encroachment over 70 years in South African savannahs: overgrazing, global change or extinction aftershock? Philos. Trans. R. Soc. B Biol. Sci. 371, 20150437. doi:10.1098/rstb.2015.0437

Sulla-Menashe, D., Friedl, M.A., 2018. User Guide to Collection 6 MODIS Land Cover (MCD12Q1 and MCD12C1) Product, 1–18. doi:10.5067/MODIS/MCD12Q1

Svoray, T., Karnieli, A., 2011. Rainfall, topography and primary production relationships in a semiarid ecosystem. Ecohydrology 4, 56–66. doi:10.1002/eco

Thornton, P.K., van de Steeg, J., Notenbaert, A., Herrero, M., 2009. The impacts of climate change on livestock and livestock systems in developing countries: A review of what we know and what we need to know. Agric. Syst. 101, 113–127. doi:10.1016/j.agsy.2009.05.002

Tian, F., Brandt, M., Liu, Y.Y., Rasmussen, K., Fensholt, R., 2017. Mapping gains and losses in woody vegetation across global tropical drylands. Glob. Chang. Biol. 23, 1748–1760. doi:10.1111/gcb.13464

Tian, F., Brandt, M., Liu, Y.Y., Verger, A., Tagesson, T., Diouf, A.A., Rasmussen, K., Mbow, C., Wang, Y., Fensholt, R., 2016. Remote sensing of vegetation dynamics in drylands: Evaluating vegetation optical depth (VOD) using AVHRR NDVI and in situ green biomass data over West African Sahel. Remote Sens. Environ. 177, 265–276. doi:10.1016/j.rse.2016.02.056

Tong, X., Brandt, M., Yue, Y., Horion, S., Wang, K., Keersmaecker, W. De, Tian, F., Schurgers, G., Xiao, X., Luo, Y., Chen, C., Myneni, R., Shi, Z., Chen, H., Fensholt, R., 2018. Increased vegetation growth and carbon stock in China karst via ecological engineering. Nat. Sustain. 1, 44–50. doi:10.1038/s41893-017-0004-x

UN DESA, 2019. World Population Prospects: Volume I: Comprehensive Tables (ST/ESA/SER.A/426), World Population Prospects. New York, USA. doi:10.18356/cd7acf62-en

van Ittersum, M.K., van Bussel, L.G.J., Wolf, J., Grassini, P., van Wart, J., Guilpart, N., Claessens, L., de Groot, H., Wiebe, K., Mason-D'Croz, D., Yang, H., Boogaard, H., van Oort, P.A.J., van Loon, M.P., Saito, K., Adimo, O., Adjei-Nsiah, S., Agali, A., Bala, A., Chikowo, R., Kaizzi, K., Kouressy, M., Makoi, J.H.J.R., Ouattara, K., Tesfaye, K., Cassman, K.G., 2016. Can sub-Saharan Africa feed itself? Proc. Natl. Acad. Sci. 113, 14964–14969. doi:10.1073/pnas.1610359113

Veldman, J.W., Aleman, J.C., Alvarado, S.T., Anderson, T.M., Archibald, S., Bond, W.J., Boutton, T.W., Buchmann, N., Buisson, E., Canadell, J.G., Dechoum, M. de S., Diaz-Toribio, M.H., Durigan, G., Ewel, J.J., Fernandes, G.W., Fidelis, A., Fleischman, F., Good, S.P., Griffith, D.M., Hermann, J.M., Hoffmann, W.A., Stradic, S.L., Lehmann, C.E.R., Mahy, G., Nerlekar, A.N., Nippert, J.B., Noss, R.F., Osborne, C.P., Overbeck, G.E., Parr, C.L., Pausas, J.G., Pennington, R.T., Perring, M.P., Putz, F.E., Ratnam, J., Sankaran, M., Schmidt, I.B., Schmitt, C.B., Silveira, F.O.A., Staver, A.C., Stevens, N., Still, C.J., Strömberg, C.A.E., Temperton, V.M., Varner, J.M., Zaloumis, N.P., 2019. Comment on "The global tree restoration potential". Science. 366, 1–5. doi:10.1126/science.aaz0111

Venter, Z.S., Cramer, M.D., Hawkins, H.J., 2018. Drivers of woody plant encroachment over Africa. Nat. Commun. 9, 1–7. doi:10.1038/s41467-018-04616-8

Venter, Z.S., Hawkins, H.J., Cramer, M.D., 2017. Implications of historical interactions between herbivory and fire for rangeland management in African savannas. Ecosphere 8, 1–14. doi:10.1002/ecs2.1946

Wei, F., Wang, S., Brandt, M., Fu, B., Meadows, M.E., Wang, Lixin, Wang, Lanhui, Tong, X., Fensholt, R., 2020. Responses and feedbacks of African dryland ecosystems to environmental changes. Curr. Opin. Environ. Sustain. 48, 29–35. doi:10.1016/j.cosust.2020.09.004

Wessels, K.J., Prince, S.D., Malherbe, J., Small, J., Frost, P.E., VanZyl, D., 2007. Can human-induced land degradation be distinguished from the effects of rainfall variability? A case study in South Africa. J. Arid Environ. 68, 271–297. doi:10.1016/j.jaridenv.2006.05.015

White, F., 1983. The vegetation of Africa: a descriptive memoir to accompany the Unesco/AETFAT/UNSO vegetation map of Africa (Natural Resources Research: 20). Paris: United Nations Educational, Scientific and Cultural Organization

White, R., Murray, S., Rohweder, M., 2000. Grassland Ecosystems. Washington, DC

Wigley, B.J., Bond, W.J., Hoffman, M.T., 2010. Thicket expansion in a South African savanna under divergent land use: Local vs. global drivers? Glob. Chang. Biol. 16, 964–976. doi:10.1111/j.1365-

2486.2009.02030.x

Wu, Z., Ahlström, A., Smith, B., Ardö, J., Eklundh, L., Fensholt, R., Lehsten, V., 2017. Climate data induced uncertainty in model-based estimations of terrestrial primary productivity. Environ. Res. Lett. 12. doi:10.1088/1748-9326/aa6fd8

Zaehle, S., Sitch, S., Smith, B., Hatterman, F., 2005. Effects of parameter uncertainties on the modeling of terrestrial biosphere dynamics. Global Biogeochem. Cycles 19, 1–16. doi:10.1029/2004GB002395

Zhang, W., Brandt, M., Penuelas, J., Guichard, F., Tong, X., Tian, F., Fensholt, R., 2019. Ecosystem structural changes controlled by altered rainfall climatology in tropical savannas. Nat. Commun. 10. doi:10.1038/s41467-019-08602-6

Zhu, L., Southworth, J., 2013. Disentangling the relationships between Net primary production and precipitation in Southern Africa savannas using satellite observations from 1982 to 2010. Remote Sens. 5, 3803–3825. doi:10.3390/rs5083803

Zhu, Z., Piao, S., Myneni, R.B., Huang, M., Zeng, Z., Canadell, J.G., Ciais, P., Sitch, S., Friedlingstein, P., Arneth, A., Cao, C., Cheng, L., Kato, E., Koven, C., Li, Y., Lian, X., Liu, Y., Liu, R., Mao, J., Pan, Y., Peng, S., Peñuelas, J., Poulter, B., Pugh, T.A.M., Stocker, B.D., Viovy, N., Wang, X., Wang, Y., Xiao, Z., Yang, H., Zaehle, S., Zeng, N., 2016. Greening of the Earth and its drivers. Nat. Clim. Chang. 6, 791–795. doi:10.1038/nclimate3004